STRUCTURAL AND FUNCTIONAL BRAIN ABNORMALITIES IN CHILDREN WITH FETAL ALCOHOL SPECTRUM DISORDERS (FASD)

A THESIS
SUBMITTED TO THE FACULTY OF THE GRADUATE SCHOOL
OF THE UNIVERSITY OF MINNESOTA
BY

JEFFREY ROBERT WOZNIAK

IN PARTIAL FULFILLMENT OF THE REQUIREMENTS
FOR THE DEGREE OF
MASTER OF SCIENCE

KELVIN O. LIM, M.D., ADVISER

MAY, 2011

Acknowledgements

I would like to acknowledge the contributions of my mentor and adviser, Kelvin O. Lim, M.D., my other committee members S. Charles Schulz, M.D. & Monica Luciana, Ph.D., and my many collaborators without whom this work would not have been possible: Bryon A. Mueller, Ryan L. Muetzel, Heather L. Hoecker, Melesa A. Freerks, Pi-Nian Chang, Lydia Caros, Erin E. Ward, Christopher J. Bell, Miranda L. Nelson, and Christie L. McGee.

Dedication

This thesis is dedicated to the many children and families affected by Fetal Alcohol Spectrum Disorders who took the time to participate in this research. I am grateful for all of your substantial contributions.

ABSTRACT

Over the past five years, Diffusion Tensor Imaging (DTI) has begun to provide new evidence about the effects of prenatal alcohol exposure on white matter development. DTI, which examines microstructural tissue integrity, is more sensitive to subtle white matter abnormalities than traditional volumetric MRI methods. Thus far, the available DTI data suggest that white matter microstructural abnormalities fall on a continuum of severity in Fetal Alcohol Spectrum Disorder (FASD). Abnormalities are prominent in the corpus callosum, but also evident in major anterior-posterior fiber bundles, corticospinal tracts, and cerebellum. These subtle abnormalities are correlated with neurocognitive deficits, especially in processing speed, non-verbal ability, and executive functioning.

The two studies presented here provide evidence of microstructural anomalies in the brains of children who were prenatally exposed to alcohol and demonstrate that those anomalies are associated with disruptions in functional brain connectivity. The majority of the patients in these two investigations were children who did not meet full criteria for Fetal Alcohol Syndrome (FAS). Thus, these data provide evidence that there are genuine consequences of moderate alcohol consumption during pregnancy even in the absence of the full syndrome. Ultimately, these types of sensitive brain measures may serve as indices of change in future longitudinal studies and in studies of interventions for FASD.

Table of Contents

Section	Page
List of tables……	v
List of figures..……	vi
Introduction……..…….....	1
Study #1……	17
Methods……	17
Results……..	25
Discussion……	27
Study #2……	33
Methods……	34
Results…….	45
Discussion……	49
Conclusion……	56
Bibliography……	58

List of Tables

Table	Page
Table 1. Summary of published DTI findings and effect sizes in FASD specifically highlighting abnormalities in the corpus callosum	15
Table 2. Subject characteristics for FASD and control groups	20
Table 3. Means, standard deviations (SD), and univariate test results (following MANOVA) for fractional anisotropy (FA) and mean diffusion (MD) in six corpus callosum tracts	25
Table 3. Subject characteristics for FASD and control groups	38
Table 4. MRI sequence and parameters	39
Table 5. Corpus callosum regions of interest (ROIs), corresponding cortical regions to which fibers project, and associated FreeSurfer grey matter ROIs at the distal ends of the white matter tracts	43

List of Figures

Figure	Page
Figure 1. Illustration of *isotropic* and *anisotropic* diffusion	3
Figure 2. Raw diffusion images and fractional anisotropy maps	4
Figure 3. Semi-automated delineation of six corpus callosum regions of interest (ROIs)	23
Figure 4. Six inter-hemispheric connectivity distribution masks (tracts) generated by tractography.	24
Figure 5. Illustration of the relationship between the isthmus corpus callosum tract and the corresponding set of para-central cortical regions of interest.	43
Figure 6. Sample six-minute resting fMRI time-series from two participants recorded from left and right medial orbital-frontal regions of interest.	44
Figure 7. Inter-hemispheric connectivity by group (control vs. FASD) for four cortical regions of interest.	45
Figure 8. Inter-hemispheric connectivity in the para-central region by diagnostic group.	46

INTRODUCTION

Prenatal alcohol exposure represents a major public health problem that results in permanent neurodevelopmental abnormalities for a very large number of individuals. The incidence of full Fetal Alcohol Syndrome (FAS) is approximately 0.1% of the population, but a much larger group of individuals experiences the damaging effects of prenatal alcohol exposure (Abel, 1995). Epidemiologic data suggest that the incidence of Fetal Alcohol Spectrum Disorders (FASD) is as high as 0.9% of the population (Lupton et al., 2004; May and Gossage, 2001; Sampson et al., 1997).

In the past five years, a series of brain imaging studies using Diffusion Tensor Imaging (DTI) has deepened our understanding of the neurodevelopmental effects of prenatal alcohol exposure. It has been known for some time that prenatal alcohol exposure is associated with serious cognitive consequences including low IQ, attention and executive functioning deficits, memory impairments, visual-spatial abnormalities, and fine motor deficits among others (Mattson & Riley, 1998). These problems occur across the FASD spectrum as evidenced by studies showing cognitive deficits in children who were prenatally exposed to alcohol, regardless of whether they met the full diagnostic criteria for FAS (Larroque and Kaminski, 1998; Mattson et al., 1997; Olson et al., 1997; Testa et al., 2003).

Earlier neuroimaging studies demonstrated that gross structural brain anomalies were common in FAS, a diagnosis that is made on the basis of heavy prenatal alcohol exposure, growth deficiency, dysmorphic facial features, and serious cognitive impairment. DTI may be uniquely suited to the study of a broader range of effects due to

prenatal alcohol exposure known as FASD because it is non-invasive, it is sensitive to normal brain development, and it provides measures of tissue organization and integrity at a microscopic level not achievable with conventional volumetric MRI methods.

Thus far, despite differences in populations and methodologies across studies, DTI studies have provided relatively consistent results in major white matter tracts, including the corpus callosum, in FASD. The findings demonstrate that subtle white matter disruption may be an important neurodevelopmental component of FASD and highlight the need for a more complete understanding of the cognitive consequences of white matter disturbance during brain development.

A brief overview of DTI methods

DTI is a Magnetic Resonance Imaging (MRI) technique that measures the diffusion of water molecules in tissue (Le Bihan, 1995; Stejskal & Tanner, 1965). Molecules that are unrestricted by tissue structure diffuse via Brownian motion in an *isotropic* manner – equally in all planes (see Figure 1). In tissue, the orientation of the diffusion is often differentially restricted, such as by cell membranes, fibers, and myelin (Moseley et al., 1990). For example, in white matter, the diffusion occurs more readily parallel to the axons rather than perpendicular to the axons. This orientation-specific diffusion is called *anisotropic* (Beaulieu, 2002).

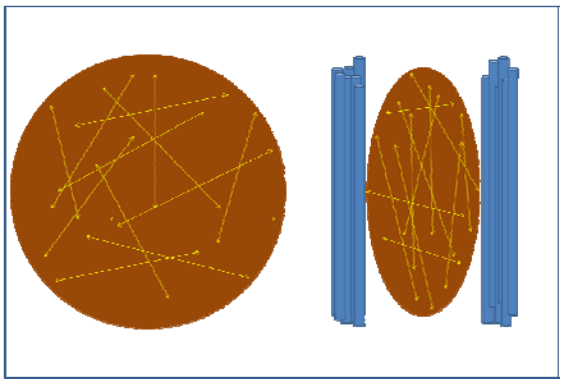

Figure 1. The panel on the left illustrates *isotropic* diffusion which is equal in all orientations. Diffusion is more *isotropic* in tissue that contains few or no restrictions. The panel on the right illustrates *anisotropic* diffusion which is orientation-specific. Diffusion is more *anisotropic* in structured tissue such as white matter fiber bundles.

DTI measures the orientation and magnitude of diffusion in three dimensions and subsequently reconstructs the data into a three-dimensional volume, (Basser, Mattiello, & LeBihan, 1994b), allowing for mapping of white matter structure as well as measurement of tissue "integrity" on a voxel-by-voxel level. The tensor in DTI simply refers to a mathematical construct for representing the magnitude of water diffusion in three-dimensional space (Basser & Pierpaoli, 1996).

Following data acquisition, a diffusion tensor matrix is constructed and matrix diagonalization is used to compute three eigenvectors (Basser & Pierpaoli, 1998). Scalar measures are derived from the eigenvectors. The sum total of the three eigenvalues ($\lambda_1 + \lambda_2 + \lambda_3$) is the defined as the *trace* of the diffusion tensor. The average of the three eigenvalues is the *mean diffusivity* (MD). In white matter, the first and largest of the eigenvalues, λ_1 , represents diffusivity parallel to the axons and is referred to as the *axial diffusivity* (Basser, 1995) or *parallel diffusivity*. Similarly, the second and third eigenvalues, λ_2 and λ_3 , represent diffusivity in the planes orthogonal to the axons and are

usually averaged $(\lambda_2 + \lambda_3)/2$, resulting in a measure of *radial diffusivity* or *perpendicular diffusivity*. The most commonly reported measure, *fractional anisotropy* (FA), represents the fraction tensor's magnitude that is due to anisotropic diffusion (Basser, Mattiello, & LeBihan, 1994a; Masutani, Aoki, Abe, Hayashi, & Otomo, 2003). Abnormal brain development or acquired brain damage typically contributes to lower FA and higher MD values in affected white matter compared with normal white matter (Neil, Miller, Mukherjee, & Huppi, 2002). Figure 2 contains examples of fractional anisotropy maps, color-coded to show the orientation of major white matter fiber bundles.

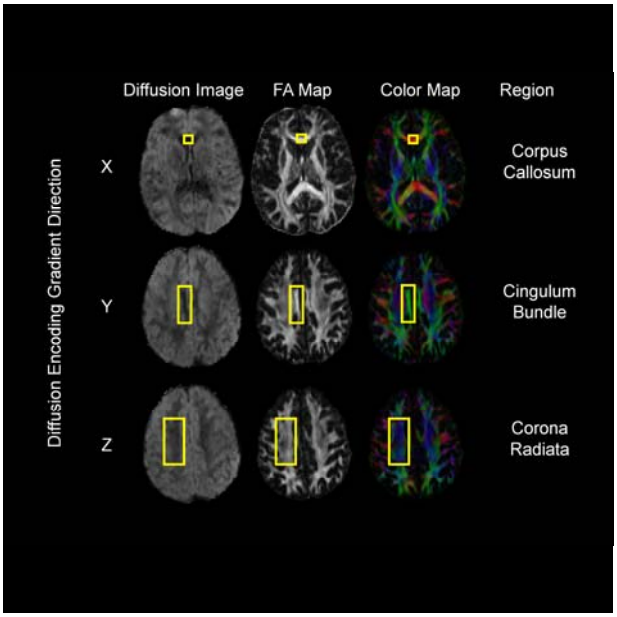

Figure 2. The first column illustrates raw diffusion-weighted images with diffusion weighting applied in "X" (left-right), "Y"(anterior-posterior), and "Z" (superior-inferior) planes. Signal attenuation (dark regions) is the result of water diffusion in the plane of the diffusion encoding gradient. The second column shows fractional anisotropy (FA) maps at the same slices. The third column shows diffusion encoded color maps, where red indicates diffusion in "X", green indicates diffusion in "Y", blue indicates diffusion in "Z", and combinations of the colors indicates diffusion in combinations of "X", "Y", and/or "Z". Yellow boxes highlight structures within each image to illustrate signal attenuation in the diffusion images and the corresponding color encoding in the diffusion encoded color maps.

Currently, the physiological meaning of DTI measures such as FA and MD is not yet fully understood (for a review, see (Beaulieu, 2009)). With the recent publication of numerous DTI studies, it has now become clear that DTI does not measure a *single* characteristic of white matter development or integrity. Rather, DTI reflects underlying aspects of tissue organization at numerous levels (Neil, et al., 2002). Although DTI is often thought to predominantly reflect myelin status, it is clear that DTI is sensitive to several aspects of axonal integrity as well as the general organization and alignment of groups of axons and fibers in white matter tissue (Beaulieu, 2002; Neil, et al., 2002). Thus, although DTI is sensitive to the type of damage caused by prenatal alcohol exposure, it seems unlikely that DTI by itself will be able to substantially increase our understanding of the actual physiological mechanisms of alcohol damage in the brain.

In addition, as a further caveat in understanding the strengths and limitations of DTI, a detailed example illustrating the scale of the measurements is worthwhile (Wozniak, Mueller, & Lim, 2008): Free water molecules diffuse an average of 10 microns during a typical diffusion encoding sequence (Le Bihan, 2003; Mori & Zhang, 2006). Axons in the corpus callosum have a median diameter of about 1 micron with a range of 0.2 to 10 microns (Aboitiz, Scheibel, Fisher, & Zaidel, 1992). The actual spatial resolution of the DTI image is many orders of magnitude larger than the scale of the individual axon. For example, a common DTI *voxel* (a single three-dimensional '**vo**lume pi**xel**' in the image) is 2.5 x 2.5 x 2.5 millimeters, or 2500 microns per side and 6.25 million square microns in cross-section. Thus, the measured diffusion in a single corpus callosum voxel is the result of millions of axons that pass through that single voxel. Even

at 1.0 x 1.0 x1.0 millimeters, there are still approximately one million axons passing through the voxel. Therefore, despite the impressive images that DTI produces and the fact that it measures aspects of microstructural integrity, DTI remains a relatively blunt tool in our investigation of the brain.

In addition, despite the proliferation of DTI papers and software tools, DTI remains a highly technically challenging methodology with many opportunities for errors and biases along the complex path from data acquisition to processing to final analysis (Jones & Cercignani, 2010). Nonetheless, with a clear understanding of the limitations of the technique, it remains evident that DTI is a promising tool that has now become a staple in the investigation of a wide range of neurodevelopmental conditions (Alkonyi et al., 2010; Cykowski, Fox, Ingham, Ingham, & Robin, 2010; Filippi et al., 2003; Groen, Buitelaar, van der Gaag, & Zwiers, 2010; Kao, Peng, Weng, Lin, & Lee, 2010; Kumar et al., 2010; Mullen et al., 2010; Radua, Via, Catani, & Mataix-Cols, 2010; Shukla, Keehn, & Muller, 2010; Utsunomiya, 2010; Wozniak, Mueller, Ward, Lim, & Day, in press; Yoshida et al., 2010). Ultimately, DTI's primary advantage lies in its sensitivity: to neurodevelopmental abnormalities, to normal developmental changes, to changes in disease status including progression and recovery (Teipel et al., 2010; Wu et al., 2010), and to the effects of both biological and behavioral treatments (Fox et al., 2010; Keller & Just, 2009; Schweder et al., 2010; Trivedi et al., 2008). As we move into the era of new interventions for FASD, including micronutrient supplementation and others, the availability of sensitive, non-invasive measures of brain status – like DTI – will become increasingly important.

The role of white matter in the brain: context for DTI studies of FASD

Cerebral white matter is made up of three major types of fibers: *commissural fibers* (including the corpus callosum, anterior and posterior commissures, and hippocampal commissure) that connect corresponding regions in the right and left hemispheres; *association fibers* that connect regions within the same hemisphere, locally across long distances; and *projection fibers* that connect cortex to deep gray matter structures. White matter's appearance is largely due to myelin, the fatty layer that surrounds axons. Myelination of axons is essential for efficient neural transmission. Myelination unfolds as part of an orderly developmental sequence: posterior regions are myelinated prior to anterior regions (Barkovich, Kjos, Jackson, & Norman, 1988; Hayakawa, Konishi, Kuriyama, Konishi, & Matsuda, 1991; Kinney, Brody, Kloman, & Gilles, 1988). In the cerebrum, myelination occurs rapidly and broadly during the prenatal period and into the second year of life; it continues more slowly into adolescence and young adulthood (Holland, Haas, Norman, Brant-Zawadzki, & Newton, 1986). Long fibers, including those that bridge the two hemispheres, are myelinated first, followed by the shorter inter-cortical associational neurons (Yakolev & Lecours, 1967). The final stages of myelination occur in the frontal lobes during adolescence, accompanied by significant cognitive growth, especially in executive functioning.

Although historically white matter has been thought to be primarily important for motor and sensory functioning, more recent conceptualizations suggest that white matter's principal role may be to serve as the infrastructure of the brain's neural networks. Thus, white matter is critical for complex high-level cognitive processes

involving attention, executive functioning, non-verbal / visual-spatial processing, and speed (Filley, 1998; Geschwind, 1965). Data from numerous studies of white matter diseases including Multiple Sclerosis (Rao, 1995), toxic leukoencephalopathy (Filley & Kleinschmidt-DeMasters, 2001), cerebral autosomal dominant arteriopathy with subcortical infarcts and leukoencephalopathy (CADASIL), and others (Pantoni & Garcia, 1995) provide direct evidence that intact white matter is necessary for normal executive function, attention, processing speed, and motor skill (Sullivan & Pfefferbaum, 2011). White matter integrity, as measured by DTI, has also been shown to be associated with working memory, processing speed, and attention in adults with alcoholism (Chanraud, Zahr, Sullivan, & Pfefferbaum, 2010; Pfefferbaum et al., 2000). Processing speed deficits have also been associated with DTI abnormalities in children with shear-damaged white matter as a result of traumatic brain injury (TBI) (Wilde et al., 2006). Similarly, Wozniak et al. (2007) showed associations between DTI measures of white matter damage and both attention and executive functioning deficits in children with TBI. Thus, DTI appears to be sensitive to the kind of underlying brain damage that is known to contribute to the types of cognitive deficits frequently observed in FASD.

White matter macrostructure in FASD

Before the advent of DTI, a number of studies using macrostructural methods demonstrated white matter abnormalities in FASD. Riley et al. (1995) showed smaller corpus callosum area in prenatally-exposed individuals, even after correcting for smaller brain size. Archibald et al. (2001) reported white matter hypoplasia, especially in the

parietal region, in subjects with histories of prenatal alcohol exposure. In a study using voxel-based morphometry, Sowell et al. reported lower white matter density in left posterior temporo-parietal cortex, a region that is connected inter-hemispherically by posterior callosal fibers (Sowell, Thompson, et al., 2001). In another study, Sowell et al. did not observe lower callosal area after adjusting for brain size, but did report highly significant alterations in callosal shape in prenatally-exposed subjects (Sowell, Mattson, et al., 2001). Specifically, they reported displacement of the callosum, primarily in the posterior regions (isthmus and splenium). Moderate correlations were observed between callosal shape abnormalities and performance on cognitive measures, including a verbal learning measure. Callosal shape abnormalities have also been reported in FAS and Fetal Alcohol Effects (FAE) in a series of studies (Bookstein, Sampson, Connor, & Streissguth, 2002; Bookstein, Sampson, Streissguth, & Connor, 2001; Bookstein, Streissguth, Sampson, Connor, & Barr, 2002). Bookstein et al. (2002) also demonstrated relationships between callosal shape disruption and cognition. Specifically, they reported that higher callosal thickness was associated with executive functioning deficits whereas lower callosal thickness was associated with motor abnormalities. A significant relationship between callosal volume and performance on a finger localization task (which is dependent on callosal transfer) has also been shown in FASD (Roebuck, Mattson, & Riley, 2002). Slower inter-hemispheric transfer of information was associated with lower callosal volume. Overall, the evidence for macrostructural abnormalities in FASD, especially in the more severe forms such as FAS, led to the

search for more subtle microstructural abnormalities across the full spectrum using methods such as DTI.

DTI findings in Fetal Alcohol Spectrum Disorders: The first five years

The first DTI study of FASD (Ma et al., 2005) examined adults (ages 18-25) with FAS. The study involved measurements of fractional anisotropy (FA) and apparent diffusion coefficient (ADC) (also called Mean Diffusivity (MD)) from hand-drawn regions of interest (ROIs) in the genu and splenium of the corpus callosum at the mid-sagittal slice. Lower FA and higher MD were found in both ROIs for the FAS group compared with controls, suggesting microstructural abnormalities in the alcohol-exposed brains. No correlations between DTI measures and facial dysmorphia were observed. Although higher FA in the genu was correlated with faster processing speed in controls, there was no significant correlation in the FASD group. The correlations between FA measures and full-scale IQ were not significant in either group.

Wozniak et al. (2006) examined children with mild to moderate severity FASD (none had FAS), ages 10 to 13, using DTI and found predominantly posterior corpus callosum abnormalities among six midline ROIs that were examined. Specifically, higher MD was seen in the isthmus region for children with FASD compared with control subjects. None of the DTI metrics was found to be associated with the degree of facial dysmorphology.

Using a voxel-wise approach, Sowell et al. (2008) found lower FA in children with FASD (ages 7 to 15). Lower FA was seen in several regions including the right and

left lateral aspects of the splenium, although not at the midline (primarily in superior parietal regions). In that study, lower FA in the lateral splenium was associated with lower performance on a measure of visuomotor skill among the children with FASD. Other regions in which the FASD group showed lower FA included bilateral posterior cingulate, right temporal lobe (inferior longitudinal fasciculus and inferior fronto-occipital fasciculus), right internal capsule, and brainstem. No significant relationship between reading ability and white matter status was observed.

Lebel et al. (2008) used a semi-automated DTI tractography method in children with FASD (ages 5 to 12). Compared with controls, the FASD group had lower FA in the splenium tract and lower MD for the tract involving the genu. The finding of lower MD in the genu among those with FASD is noteworthy because lower MD is thought to reflect a higher degree of fiber coherence / organization and this finding contrasted the Ma et al. (2005) study. Group differences in DTI measures were also seen in a number of other white matter and grey matter regions including bilateral inferior and superior longitudinal fasciculi, right cingulum, bilateral globus pallidus, and left thalamus. In this study, no significant correlations were observed between the DTI metrics and measures of executive functioning, working memory, reading, vocabulary, or mathematical ability.

Fryer et al. (2009) examined white matter in a group of children (ages 8 to 18) with heavy prenatal alcohol exposure compared with controls using Tract-Based Spatial Statistics (TBSS) (Smith et al., 2006), a voxel-wise method that focuses on central white matter voxels in order to minimize the effects of inter-subject registration problems. They reported lower FA in a significant number of white matter tracts including right

superior longitudinal, uncinate, and fronto-occipital fasciculi, bilateral anterior/superior corona radiata, bilateral posterior corona radiata, and bilateral forceps major. The abnormalities were most prominent in the medial regions of frontal and occipital lobes. They also observed low FA in the body of the corpus callosum. Although FA in each of these white matter regions distinguished the FASD group from controls, only FA in the body of the callosum distinguished those with FAS from those with prenatal exposure to alcohol (PEA). Thus, DTI measures in midline structures, such as the corpus callosum, may reflect severity and, perhaps the extent of the alcohol exposure. Despite a preponderance of regions that showed lower FA in subjects with alcohol exposure relative to control subjects, there were some regions -- including the right cingulum and right posterior limb of the internal capsule -- in which the opposite (higher FA) was observed in the alcohol-exposed group. These somewhat counterintuitive findings and those of Lebel cited above should be evaluated in the context of evidence that higher than normal FA and lower than normal MD could be indicative of pathology such as damage to regions of crossed fibers (which normally have very low FA and high MD) for example. Alternatively, such findings could be related to other developmental insults that commonly co-occur with FASD. For example, high FA and low MD have been seen in samples of individuals with prenatal exposure to tobacco and other drugs, as discussed in detail in a section below.

In another study employing a TBSS examination of the corpus callosum among adults with FASD (ages 19 to 27), Li et al. (2009) reported lower FA, higher MD, and higher radial diffusivity (RD) in the isthmus for individuals with dysmorphic facial

features compared with controls. Significant group differences in FA were also seen in the splenium. These abnormalities were at the midline but they also extended into the lateral callosal fibers. There were no statistically significant differences between the FASD group without dysmorphic facial features and controls, but the FA, MD, and radial diffusivity (RD) values fell between the other two groups, suggesting a continuum of effects. Correlations between the DTI measures and full-scale IQ as well as facial dysmorphia ratings were non-significant.

In a study utilizing DTI tractography, Wozniak et al. (2009) examined the integrity of corpus callosum tracts at the midline and extending into the cerebral hemispheres in children with FASD (ages 10 to 17) (see Study #1). FA in the inter-hemispheric fibers of the posterior midbody, isthmus, and splenium of the corpus callosum was significantly lower in the FASD group compared with controls. No significant correlation was found between the DTI measures of white matter integrity and facial dysmorphology. In the FASD group, a significant correlation was observed between the Wechsler Working Memory Index and FA in the genu but not FA in the splenium. Similarly, significant correlations were seen between MD in the splenium and both the Working Memory and Perceptual Organizational indices. There were no associations between Perceptual Organization and the DTI measures in the genu. Although the findings do not represent a double dissociation, they do indicate a degree of regional specificity.

Recently, Lebel et al. (2010) used a voxel-wise approach to examine relationships between white matter DTI measures and math ability in a sample of children with FASD

(ages 5 to 13). They observed significant associations between FA and math ability in the left cerebellum, left parietal lobe, and bilateral brainstem after controlling for age. Fiber tracking revealed that the significant parietal clusters were part of the superior longitudinal fasciculus, a tract known to be related to overall cognitive functioning and to math ability in particular.

As an illustration of the relative consistency of DTI evidence of white matter abnormalities in individuals with FASD thus far, Table 1 provides a summary of findings specifically highlighting the corpus callosum. For purposes of comparison, Cohen's d effect sizes were computed for the studies that used defined ROIs. Variability in findings across studies may be related to differences in age, diagnosis, severity, sample size, and DTI methodology. As would be expected, the largest group effect sizes come from the study of the most severely affected population, those with FAS and mean IQ = 58 (Ma, et al., 2005), but moderate effects are also evident in less severely affected individuals on the FASD spectrum.

Looking across studies, it is apparent that microstructural abnormalities occur throughout the corpus callosum (as well as elsewhere in the brain) but are most consistently seen in the posterior regions of the callosum – especially in the isthmus and splenium. In evaluating the various methods of data analysis used in these studies, it is apparent that ROI-based methods have significant power to discriminate groups, voxel-wise analyses are useful for characterizing the extent of the effects across the whole brain, and tractography methods are essential in moving forward to better understand the specific functional implications of these structural effects. Overall, these studies

consistently demonstrate that DTI is sensitive to white matter abnormalities in FASD, including those who do not meet full criteria for FAS.

Table 1. Summary of published DTI findings and effect sizes in FASD specifically highlighting abnormalities in the corpus callosum.

Study	Population	Method	Cohen's d effect size	% difference
Ma et al. (2005)	Controls vs. adults (ages 18-25) with FAS, mean IQ = 58	Two hand-drawn mid-sagittal ROIs	Genu: MD = 2.39 FA = -3.11 Splenium: MD = 1.91 FA = -2.98	Genu: MD = 14.3% FA = 25.6% Splenium: MD = 16.6% FA = 14.9%
Wozniak et al. (2006)	Controls vs. children (ages 10-13) with FASD (non-FAS), mean IQ = 89	Six hand-placed mid-sagittal ROIs	Genu: MD = 0.21 FA = -0.25 Splenium: MD = 0.07 FA = -0.31 Isthmus: MD = 1.05 FA = -0.42	Genu: MD = 1.7% FA = 2.2% Splenium: MD = 0.9% FA = 2.9% Isthmus: MD = 15.2% FA = 6.6%
Sowell et al. (2008)	Controls vs. children (ages 7-15) with FASD, mean IQ = 89	Voxel-wise analysis with post-hoc ROI analysis.	Right lateral splenium: FA: -1.20 Left lateral splenium: FA: -1.17	Right lateral splenium: FA: 15.8% Left lateral splenium: FA: 17.7%
Lebel et al. 2008	Controls vs. children (ages 5-12) with FASD, mean IQ not reported	Semi-automated tractography	Genu: MD = -0.41* FA = -0.04 Splenium: MD = 0.22 FA = -0.62 Body of the callosum: MD = 0.05 FA = -0.12	Genu: MD ≈ 2.5%* FA ≈ 0% Splenium: MD ≈ 2.4% FA ≈ 3.5% Body of the callosum: MD ≈ 1.1% FA ≈ 0%
Fryer et al. (2009)	Controls vs. children (ages 8 – 18) with FASD, mean IQ = 88	Voxel-wise analysis with pos-hoc ROI analysis (Tract Based Spatial Statistics – TBSS)	Body of the callosum: FA = -1.27	N.A.
Li et al. (2009)	Controls vs. adults (ages 19-27) with FASD [effect sizes are for controls vs. FASD with facial dysmorphia (mean IQ = 78].	Voxel-wise analysis with pos-hoc ROI analysis (Tract Based Spatial Statistics – TBSS)	Genu: MD = 0.12 FA = -0.54 Splenium: MD = 0.26 FA = -2.26 Isthmus: MD = 0.72 FA = -0.75	Genu: MD = 1.7% FA = 5.2% Splenium: MD = 3.4% FA = 15.1% Isthmus: MD = 8.6% FA = 10.1%
Wozniak et al. (2009)	Controls vs. children (ages 10-17) with FASD, mean IQ = 77.	Semi-automated tractography	Genu: MD = 0.25 FA = -0.59 Splenium: MD = 0.35 FA = -0.78 Isthmus: MD = 0.24 FA = -0.72	Genu: MD = 0.9% FA = 2.8% Splenium: MD = 2.1% FA = 4.1% Isthmus: MD = 1.2% FA = 3.7%

NOTES: * MD was lower in the FASD group compared to controls, an unexpected finding.

Ultimately, as research moves forward in FASD, it will be important to begin to understand the relationships between the initial effects of alcohol on white matter tissue, the interaction of specific exposure timing and an unfolding developmental process, and the differential sensitivity of the measures at various points in brain development. The first study presented here was done in order to replicate and extend our previous findings which were among the first to show these white matter abnormalities in FASD.

Study #1: Microstructural corpus callosum anomalies in children with prenatal alcohol exposure

For Study #1, we recruited a sample including alcohol-exposed children with static encephalopathy, partial FAS, and FAS. In addition to attempting to replicate our previous findings (Wozniak et al., 2006), we also utilized tractography to build on our findings and allow for comparisons across studies. Because imaging studies of this type typically involve small samples, replication is important and will increase confidence in the findings. In the case of FASD, including a larger, more representative sample of the spectrum may also provide clarification to the findings from previous studies. Based on the macrostructural findings associated with FASD discussed above and knowledge of the regions of the corpus callosum that are connected to these cortical areas (Huang et al., 2005), we hypothesized that children with FASD would exhibit abnormalities in multiple regions of the corpus callosum, especially in posterior regions including the isthmus and splenium.

METHODS

Subjects

All subjects were ages 10 - 17. A total of 33 children with FASD were recruited from the University of Minnesota's Fetal Alcohol Spectrum Disorders Clinic. Nineteen control subjects with no prenatal alcohol exposure were also included. Control subjects were recruited from a large metropolitan area via posted advertisements in stores, laundromats, libraries and other public buildings across a diverse range of neighborhoods

with a wide range of socioeconomic level. All children with FASD were seen clinically by a pediatric psychologist and a developmental pediatrician with formal training and more than ten years experience using the 4-Digit Diagnostic System (Astley & Clarren, 2000). MRI scans were completed within one year of the examination of dysmorphic facial features. The diagnostic system classifies individuals on four criteria: 1) growth, 2) facial characteristics, 3) CNS status, and 4) alcohol exposure. Full-criteria FAS is defined by growth deficiency (<10th percentile height and weight or <3rd percentile on either), severe facial abnormalities (abnormally thin upper lip, abnormally smooth philtrum, and palpebral fissure width more than 2 SD outside mean), moderate or severe CNS impairment (microcephaly and/or cognitive deficits more than 2 SD from mean in three or more domains), and confirmed alcohol use by the mother. Partial FAS (pFAS) is characterized by at least moderate facial abnormalities (one or more of: abnormally thin upper lip, abnormally smooth philtrum, or palpebral fissure width more than 2 SD outside mean), moderate or severe CNS impairment, and confirmed alcohol use by the mother during pregnancy. Growth deficiency is not required for pFAS. Static encephalopathy – alcohol exposed is characterized by moderate or severe CNS impairment and confirmed alcohol use by the mother during pregnancy. Dysmorphic facial features and growth deficiency are not required but may be present in static encephalopathy. For all three conditions (FAS, pFAS, and static encephalopathy – alcohol exposed), confirmed maternal alcohol consumption is required at either a "high risk" level (estimated >100 mg/dl blood alcohol concentration weekly, early in pregnancy) or a lower level that is still associated with "some risk".

Male and female children and adolescents with FAS (n = 8), pFAS (n = 23), and static encephalopathy – alcohol exposed (n = 2) were included in this study. All subjects with FASD had documentation of prenatal alcohol exposure, either by the biological parent or by social service records (rank 3 or 4 using Astley & Clarren's system). If maternal alcohol use was documented specifically as daily and chronic or consisting of weekly heavy binge drinking during pregnancy, a rank of 4 was assigned. Rank 3 was assigned for cases in which heavy maternal alcohol consumption was documented but was not daily nor were binge episodes weekly. For example, documentation of several heavy binge drinking episodes during pregnancy resulted in assigning a rank of 3. For purposes of this study, subjects were not included if maternal alcohol consumption was not heavy at any point and consisted only of minimal amounts (for example, a single drink consumed on several occasions during pregnancy). Subjects for whom prenatal alcohol exposure was only suspected but was neither self-reported by the biological mother nor observed by a third party were excluded. Subjects with FASD were excluded for other prenatal drug exposure (except nicotine and caffeine). Additional exclusion criteria for all subjects (FASD and controls) were the presence of another developmental disorder (ex. Autism, Down Syndrome), very low birthweight (<1500 grams), neurological disorder, traumatic brain injury, other medical condition affecting the brain, substance abuse or dependence in the participant, or contraindications to safe MRI scanning. Control subjects were excluded for any history of prenatal substance exposure and for history of psychiatric disorder or learning disability. Table 2 contains the subject characteristics.

Table 2. Subject characteristics for FASD and control groups in Study #1.

N(%) or mean ± sd	FASD (n = 33)	Control (n =19)	Statistical Test
Age at MRI scan	12.6 ± 2.2 yrs.	12.6 ± 2.2 yrs.	t=-.008, p=.994
Gender			
Male	18 (55%)	12 (63%)	
Female	15 (45%)	7 (37%)	χ^2=.37, p=.55
Growth Deficiency (FASD only)			
Growth rating (Astley & Clarren)			
1. None	20 (61%)	-	-
2. Mild	5 (15%)	-	-
3. Moderate	2 (6%)	-	-
4. Severe	6 (18%)	-	-
Facial Features (FASD only) (Astley & Clarren ratings)			
1. None	0 (0%)	-	-
2. Mild	2 (6%)	-	-
3. Moderate	12 (36%)	-	-
4. Severe	19 (58%)	-	-
Alcohol Exposure (FASD only) (Astley & Clarren ratings)			
1. No Risk	0 (0%)	-	-
2. Unknown Risk	0 (0%)	-	-
3. Some Risk	20 (61%)	-	-
4. High Risk	13 (39%)	-	-
FASD Category (Astley & Clarren)			
Static Encephalopathy (alcohol-exposed)	2 (6%)	-	-
Partial FAS	23 (70%)	-	-
FAS	8 (24%)	-	-
Cognitive Functioning (Wechsler)			
Verbal Comprehension Index	79.5 (11.6)	106.6 (11.5)	t=8.14, p<.001
Perceptual Reasoning Index	84.8 (16.0)	107.4 (12.5)	t=5.28, p<.001
Working Memory Index	78.7 (14.8)	102.3 (8.5)	t=6.37, p<.001
Processing Speed Index	82.0 (14.4)	103.1 (12.1)	t=5.37, p<.001
Full-Scale IQ	76.9 (13.3)	107.3 (11.1)	t=8.39, p<.001

All procedures were approved by the University of Minnesota's Research Subjects' Protection Program and all subjects underwent a comprehensive informed consent procedure. Subjects were compensated with gift cards for their time.

Cognitive evaluation

All subjects were administered either the Wechsler Intelligence Scales for Children – Fourth Edition (WISC-IV) (Wechsler, 2003) (ages 10-16) or the Wechsler

Adult Intelligence Scales – Third Edition (WAIS-III) (Wechsler, 1997) (age 17) by a research technician or doctoral-level psychology trainee. Many subjects with FASD were administered the test as part of their clinical evaluation whereas others were given the test at the time of the MRI scan. Control subjects were administered the IQ test at the time of the MRI. In all cases, the MRI scan was performed within one year of the IQ test.

MRI acquisition and processing

Subjects were scanned using a Siemens 3T Trio MRI scanner with an 8-channel parallel array head coil. The scan sequence was as follows:

1. Axial DTI: the 30-direction diffusion-weighted acquisition, positioned to cover the cerebrum and as much of the cerebellum as possible. Acquisition parameters for the dual spin echo, single shot, echo planar, diffusion weighted sequence were: TR=8500 ms, TE=90 ms, 64 slices, voxel size=2x2x2 mm, FOV=256 mm^2, 1 average, GRAPPA with acceleration factor=2, b=1000 s/mm^2). Thirty-six volumes each were collected to compute the tensor: 6 images with b=0 s/mm^2 and 30 images with diffusion gradients applied in non-collinear directions (6 min.)
2. Field map: the field map was used to correct the DTI data for geometric distortion. Positioned to match the DTI acquisition. The acquisition parameters were: TR=700ms, TE=4.62 ms / 7.08 ms, 64 slices, voxel size=2x2x2 mm FOV=256^2 mm (3 min.)

Post-processing

The imaging data were processed using tools from FMRIB's software library (FSL), including the brain extraction tool (BET), linear registration tools (FLIRT), diffusion toolbox (FDT, BEDPOST, Probtrack), and dewarping tool (FUGUE). The DTI data were corrected for eddy current distortion, field maps were used to correct the resulting data for geometric distortions caused by susceptibility induced magnetic field inhomogeneity, and the diffusion tensor was then computed using FDT.

Corpus callosum parcellation and tractography

We first defined corpus callosum seed regions of interest (ROIs) using a semi-automated approach. The DTI FA map for each subject was aligned to standard space (Montreal Neurological Institute – 152 T1 mean brain) using a 12 degree of freedom affine registration. Next, a rectangular mask, three sagittal slices thick, was defined around the corpus callosum on the midline of standard-space FA map of each subject. This rectangular mask was partitioned into 6 regions based on delineations from Witelson (1989) by first manually identifying these landmarks: the anterior portion of the genu, posterior portion of the splenium, superior portion of the mid-body, inferior portion of the genu and splenium, and the boundary between the genu and rostral body. A single operator identified these landmarks for all subjects. These landmarks were used to define the mid-point, the anterior third, the posterior third and the posterior fifth of the corpus callosum. This resulted in six geometric masks (Figure 3) that were registered back to the FA map in native space using the inverse of the above mentioned 12 degree of fit alignment. Witelson's seventh region, the rostrum, was not included as a separate region

of interest due to its small size. A left-right segmentation mask was created by including voxels with FA>0.3 and a principal eigenvector with a left-right component greater than 0.95. The left-right segmentation mask was then convolved with the 6 geometric masks defined in MNI space, together yielding a highly specific parcellation of the corpus callosum into 6 Witelson ROIs. Probabilistic tractography was then performed on each subject's DTI data with the FMRIB routine Probtrack, using the 6 corpus callosum ROIs as seed regions, yielding 6 inter-hemispheric connectivity distributions or tracts for every subject (Figure 4). A threshold was applied to the connectivity distributions to generate masks, which were subsequently applied to the DTI data, allowing for computation of mean FA and MD values within each tract for each subject.

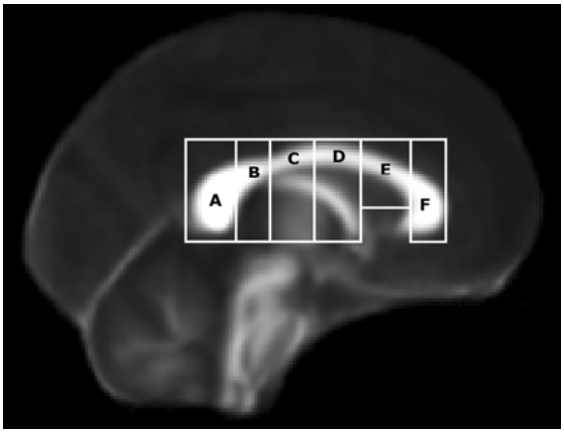

Figure 3. Six corpus callosum regions of interest (ROIs) as geometric masks, prior to being convolved with left-right segmentation maps. The regions, based on definitions from Witelson, 1989, are as follows: A.) Splenium, B.) Isthmus, C.) Posterior Midbody, D.) Anterior Midbody, E.) Rostral Body, and F.) Genu. The masks are displayed on the FMRIB 58-subject average FA map. These ROI served as the seed points for the tractography.

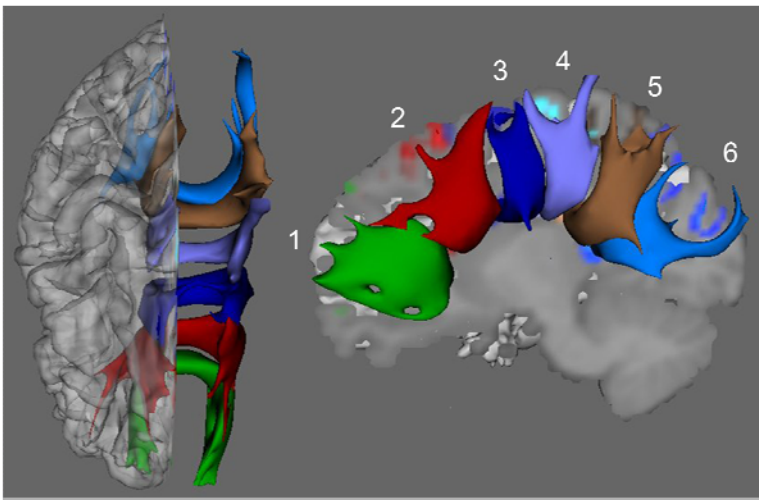

Figure 4. Six inter-hemispheric connectivity distribution masks (tracts) generated by tractography: (anterior to posterior) 1. genu; 2. rostral body; 3. anterior mid-body; 4. posterior mid-body; 5. isthmus; 6. splenium.

Reliability of the callosal segmentation and tractography method

As part of the development of our corpus callosum segmentation and tractography technique, we undertook a pilot study examining its test-retest reliability. Thirteen healthy control subjects (7 male, 6 female), ages 22-44, were scanned on the Siemens 3T Trio MRI on two separate occasions. Time between scans ranged from 1 to 29 weeks with a mean of 9.8 weeks, SD = 8.2 weeks. Fractional anisotropy (FA) was the dependent measure in this analysis. Intra-class correlations (two-way mixed model with absolute agreement for single measures) were high for all six tracts: Genu = 0.87; Rostral body = 0.86; Anterior mid-body = 0.55; Posterior mid-body = 0.63; Isthmus = 0.90; Splenium= 0.81. These findings indicate that the DTI data acquisition, post-processing, and extraction of tract-based measures are reliable, consistent with other published studies (Bonekamp et al., 2007; Heiervang et al., 2006; Wakana et al., 2007). Internal lab

data show that the manual identification of these landmarks is highly reliable (> .9) across operators.

RESULTS

Group differences

A MANOVA testing for a group difference (31 FASD vs. 19 controls) in FA across all six tracts was significant, [Wilks' Lambda = .742, F(6,45) = 2.61, p = .029]. Univariate analyses showed that the FASD group had significantly lower FA in three posterior tracts: the posterior mid-body, the isthmus, and the splenium. Effect sizes for these three tracts were large (.71, .72, and .78 respectively). A second MANOVA testing for a group difference in MD was non-significant, [Wilks' lambda =.857, F(6,43) = 1.25, p = .298]. Table 3 contains means, standard deviations, and effect sizes for FA and MD.

Table 3. Means, standard deviations (SD), and univariate test results (following MANOVA) for fractional anisotropy (FA) and mean diffusion (MD) in six corpus callosum tracts.

	FASD (*n* = 33)		**Control (*n* =19)**		**Univariate tests following MANOVA (for FA only)**		
	Mean	**SD**	**Mean**	**SD**	**F**	**p**	**Effect size (Cohen's d)**
Fractional Anisotropy (FA)							
Genu	.462	.027	.475	.016	3.55	.065	.59
Rostral Body	.429	.026	.430	.015	0.08	.779	.05
Anterior Mid-body	.424	.025	.424	.020	0.0	.986	0.0
Posterior Mid-body	.424	.026	.441	.022	6.05	.017	.71
Isthmus	.431	.025	.447	.019	5.59	.022	.72
Splenium	.462	.030	.481	.017	6.64	.013	.78
Mean Diffusivity (MD) x 10 $^{-3}$							
Genu	.879	.038	.871	.024			.25
Rostral Body	.893	.040	.881	.024			.36
Anterior Mid-body	.921	.037	.927	.033			-.17
Posterior Mid-body	.912	.047	.905	.028			.18
Isthmus	.955	.059	.967	.038			-.24
Splenium	.895	.064	.876	.043			.34

NOTES: *p<.05; Mean Diffusivity values are x10 $^{-3}$ mm^2 / second.
Univariate test statistics for MD are not listed because the overall MANOVA for MD was non-significant.

Dysmorphic facial characteristics

Data from our initial DTI study showed no relationship between dysmorphic features and mid-sagittal MD in the isthmus region (Wozniak et al., 2006). We conducted similar analyses with data from this second study in the three corpus callosum regions that showed group differences: posterior mid-body, isthmus, and splenium. Spearman correlations comparing facial dysmorphology (Astley & Clarren 1-4 rating) with FA and MD in these three regions for children with FASD were all non-significant, the highest correlation being only 0.14. Because the distribution of facial ratings was skewed (Table 2), the power of these correlational analyses was somewhat limited. As a further exploration of these relationships, we conducted independent-samples t-tests for FA and MD for the three corpus callosum regions, comparing the two largest rating categories: moderate facial features (36%) vs. severe facial features (58%). None of these t-tests was significant and there were no noteworthy trends in these comparisons.

Cognitive functioning

As expected, the FASD group performed significantly below the control group on all measures of cognitive functioning (Table 2). In order to explore the relationship between the observed corpus callosum abnormalities and cognitive functioning in those with FASD, we conducted a set of exploratory correlations between FA and MD in the anterior-most region (genu) and the posterior-most region (splenium) versus the four index scores from the Wechsler scales: Verbal Comprehension, Perceptual Organization, Working Memory, and Processing Speed in our sample of 31 FASD subjects. These

analyses were done by group to avoid inflation in the correlations from the overall group differences. The genu and splenium ROIs were chosen to limit the number of statistical tests. Due to the exploratory nature of these correlations, we examined the results without correction for the sixteen multiple comparisons. For the FASD group, a significant correlation between the Working Memory index score and FA in the genu was observed ($r = .43$, $p = .013$). Also, significant inverse correlations were observed between MD in the splenium and the Perceptual Organization index score ($r = -.45$, $p = .008$) and the Working Memory Index score ($r = -.38$, $p = .033$). There were no significant correlations between the Verbal Comprehension or Processing Speed indices and either genu or splenium FA or MD. In order to place these findings for the FASD group in context, we conducted the same set of correlations in the control group and found no significant relationships. Although these analyses are only exploratory and do not show a perfect double-dissociation, they do indicate a relationship between white matter integrity and cognition, and they suggest some regional specificity in that only posterior regions of the callosum were associated with visual-perceptual skills.

DISCUSSION

The current findings of white matter microstructural abnormalities in posterior corpus callosum are consistent with our earlier results (Wozniak et al., 2006) and with other published studies (Lebel et al., 2008; Li et al., 2009; Ma et al., 2005; Sowell et al., 2008a). Here, we report low FA in the posterior mid-body, isthmus, and splenium regions. Previously, we had observed abnormalities only in the isthmus region as

evidenced by increased MD among children with FASD compared to controls. Collectively, the available DTI literature (cited above) clearly indicates that abnormalities are present in these posterior regions, as well as elsewhere in the callosum, including the genu and the body (Fryer et al., 2009). These findings appear to be relatively consistent, but differences in diagnostic groups, sample sizes, and specific DTI methodologies employed may account for some of the differences in results across the studies. The notable difference between our 2006 finding of high MD in the isthmus and our current finding of low FA in the isthmus may be related to differences in samples and in DTI methods. The 2006 study did not include full FAS cases, whereas the current study did. In addition, the 2006 study looked at midline corpus callosum only, whereas the current study examined entire tracts projecting through the corpus callosum and into the hemispheres. The DTI methods utilized in the current study represent improvements over the methods used in our 2006 study in several respects: the current study utilized 30-direction DTI vs. 12-direction DTI in the previous study; the currently methodology is less susceptible to "edge effects" or partial-voluming effects at the boundaries of the callosum; and the current study examined larger, three-dimensional tracts as opposed to a single slice at the midline.

Thus far, in children with FASD (and in many other neurodevelopmental disorders), DTI measures are proving to be very sensitive to underlying abnormalities in tissue integrity against a background of predictable changes with normal development (Gao et al., 2008; Hasan et al., 2008; Hermoye et al., 2006; Huang et al., 2006; Qiu et al., 2008). DTI measures are also demonstrating important links between microstructural

white matter integrity and cognitive functioning in normal development (Fryer et al., 2008; Muetzel et al., 2008), acquired injuries (Wilde et al., 2006; Wozniak et al., 2007), and neurodevelopmental disorders (Alexander et al., 2007; Sundaram et al., 2008; Thakkar et al., 2008).

One challenge posed by the findings of white matter abnormalities in DTI studies of prenatal alcohol exposure is in understanding the nature of the underlying pathophysiology and its implications for individual cognition and behavior. As more DTI studies are performed in humans and in animals, we discover more about the sensitivity of the technique to different types of underlying pathology. In white matter structures such as the corpus callosum, FA values are high because the linear structure and tight packing of bundled axons restricts water molecule diffusion mostly to one direction (along the axons) (Beaulieu, 2002; J. Neil et al., 2002). Conversely, MD, which represents the mean diffusivity in all three directions, is typically low in highly organized white matter. Although myelin status plays a role in anisotropy (and is reflected in FA and MD), it is not the dominant contributing factor as made clear by studies showing significant anisotropy in unmyelinated fibers (Beaulieu & Allen, 1994a, 1994b), relatively small differences in anisotropy between myelinated and unmyelinated fibers (Gulani et al., 2001), and the presence of significant anisotropy in human newborn brains prior to major myelination stages (Huppi et al., 1998; Inder & Huppi, 2000). Although FA and MD do change predictably with brain development and are affected to an extent by changes in myelination (Beaulieu, 2002; J. J. Neil et al., 1998; Nomura et al., 1994), it is important to recognize that FA and MD are not measures of myelin status or

myelination level. In the context of a neurodevelopmental disorder such as FASD, the observed FA and MD differences may reflect structural abnormalities in the axons themselves, differences in axonal packing, differences in white matter water content, and even gross abnormalities in tract organization such as that seen in the extreme forms of agenesis and partial agenesis of the corpus callosum.

Another challenge posed by recent DTI findings in FASD is integrating these results with those from macrostructural studies of gray matter and white matter volumes, cortical thickness, and other morphometrics in FASD and, ultimately, incorporating the findings into a larger understanding of the brain damage that results from prenatal alcohol exposure. Human and animal studies examining the topography of the corpus callosum with histochemical methods or DTI (de Lacoste et al., 1985; Hofer et al., 2007; Huang et al., 2005; Matsunami et al., 1994; Pandya et al., 1971) are relatively consistent in defining the regional organization of fibers passing through the callosum. These studies suggest the following general topographic organization to the corpus callosum: orbitofrontal fibers project through the rostrum; fibers from the frontal lobe project through the genu and a large part of the anterior body of the callosum; parietal lobe fibers project through a wide portion of the posterior body of the callosum as well as the posterior-superior portion of the splenium; fibers from the temporal lobe are concentrated in the superior region of the splenium; and occipital lobe fibers are found in the inferior portion of the splenium. Thus, the consistent findings of posterior corpus callosum abnormalities in DTI studies suggest that temporal-parietal-occipital regions and associated junction regions may be of particular interest for future macrostructural and

functional studies. Relatedly, these findings suggest that additional exploration of primary visual processes, visual perception, and visual organization may be warranted in individuals with FASD.

Although the current study did not include tasks assessing primary visual processing, a general measure of visual-perception and non-verbal reasoning was available in the form of the Perceptual Reasoning Index score from the Wechsler scales. Analyses were conducted in a post-hoc, exploratory manner and, therefore, need to be considered preliminary at this point. The data, which showed a significant inverse correlation between perceptual reasoning ability and MD in the splenium and an absence of correlation with MD in the genu, suggest that DTI measures may be related to aspects of cognitive functioning that are clinically relevant to this population. These data are consistent with the findings of at least one other study which identified a relationship between white matter microstructure (FA) in the splenium and a measure of visual-motor integration (Sowell et al., 2008a). The exploratory analyses from the current study also demonstrated that higher scores on measures of working memory correlated with higher FA in the genu and lower MD in the splenium. The relationship between working memory, which many consider to be a component of executive functioning, and genu FA is intriguing, as is the unexpected finding of a potential relationship between working memory and splenium microstructural integrity. Clearly, future studies with more specific measures of neurocognitive functions will be able to expand on these results, potentially yielding new insights into the broad range of deficits observed in this population.

Lastly, we also conducted exploratory correlational analyses of the relationship between regional corpus callosum integrity and facial dysmorphology. Although midline facial anomalies and midline brain anomalies such as corpus callosum abnormalities may occur as part of the same processes during embryogenesis, there remains much to be learned about the impact of alcohol on developing organisms during gestation (Sulik, 2005). Thus far, human DTI studies in FASD are mixed with respect to the relationship between brain measures and facial dysmorphology. Our current data, together with our initial study (Wozniak et al., 2006), showed no relationship between facial characteristics and DTI measures of callosal integrity. In contrast, when comparing alcohol-exposed children with and without facial dysmorphia, Fryer et al. (2009) found that children with FAS who had dysmorphia had significantly lower FA in the midbody of the corpus callosum than those without dysmorphia. Similarly, Li et al. showed that a group of adults without dysmorphic facial characteristics fell in between the control group and a group with dysmorphic features in terms of posterior callosal FA, MD, and RD. To some extent, the specific method of characterizing and quantifying the facial abnormalities in FASD may have implications for analyses of relationships between facial dysmorphia and brain abnormalities. Future studies employing embryo models may ultimately provide the most accurate information about the link and/or independence of facial features and callosal abnormalities.

Study #2 Inter-hemispheric functional connectivity disruption in children with prenatal alcohol exposure

Having identified *microstructural* abnormalities in inter-hemispheric connectivity in FASD (Wozniak et al., 2006; Wozniak et al., 2009) (Study#1), we next sought to investigate whether inter-hemispheric *functional* connectivity is also disturbed in FASD. We were particularly interested in determining whether inter-hemispheric functional connectivity abnormalities are evident in those regions of the brain known to have underlying white matter microstructural abnormalities. Functional connectivity has been defined as the "temporal correlation between spatially remote neurophysical events" (Friston et al., 1993). Most functional connectivity studies measure brain activity during several minutes of rest and then apply correlation techniques to "map" networks in the brain based on regionally synchronized activity (Biswal et al., 1995). For example, using this innovative approach, Raichle et al. (2001) mapped a "default mode network" - a collection of brain regions not previously known to operate as a "system", and have shown that resting state networks are involved in non-task, off-line activities, perhaps including memory consolidation and planning (Raichle and Snyder, 2007). The brain's ability to coordinate itself in this fashion follows a developmental trajectory, reflected in increased functional network connectivity with age in children and young adults (Fair et al., 2008; Kelly et al., 2009). Using a number of different methods, functional connectivity has been shown to be abnormal in neurodevelopmental disorders including Autism (Broyd et al., 2008; Greicius, 2008) but there are no published studies in FASD. Inter-hemispheric connectivity has specifically been examined in a few studies. Loss of

inter-hemispheric functional connectivity has been shown in surgical severing of the callosum (Johnston et al., 2008) in epilepsy patients. Corpus callosum agenesis has also been shown to be associated with loss of inter-hemispheric functional connectivity (Quigley et al., 2003). Recently, studies have begun to demonstrate clear relationships between resting state functional connectivity and DTI measures of structural connectivity (Skudlarski et al., 2008).

For the current investigation, we hypothesized that inter-hemispheric functional connectivity would be disturbed in children with FASD and that the disturbance would be regionally specific to those areas of cortex connected by posterior corpus callosum fibers. We also hypothesized that measures of structural connectivity and functional connectivity in these regions would be associated with cognitive processes involving visual integration and visual reasoning. This study used a modified version of the semi-automated corpus callosum parcellation and tractography method that we developed and tested in Wozniak et al. (2009). This study builds on that work by simultaneously evaluating inter-hemispheric functional connectivity using a novel, straightforward method of correlating brain activity in right and left homologous cortical regions.

METHODS

Subjects

Participants were between the ages of 10 and 17. A total of 21 children with FASD were recruited from the University of Minnesota's Fetal Alcohol Spectrum Disorders Clinic. Twenty-three control subjects with no prenatal alcohol exposure were

recruited from the Twin Cities metropolitan area via advertisements on public websites, on bulletin boards, in stores, laundromats, libraries and other public buildings across a diverse range of neighborhoods, including a wide range of socioeconomic levels. As part of their clinic visit, all participants with FASD were seen by a pediatric psychologist and a developmental pediatrician with formal training and more than twelve years experience using the 4-Digit Diagnostic System (Astley and Clarren, 2000). MRI scans were completed within one year of the neurocognitive evaluation.

Astley and Clarren's diagnostic system classifies individuals on four criteria: 1) growth, 2) facial characteristics, 3) Central Nervous System (CNS) status, and 4) alcohol exposure. Full-criteria FAS is defined by growth deficiency (<10th percentile height and weight or <3rd percentile on either), severe facial abnormalities (abnormally thin upper lip, abnormally smooth philtrum, and palpebral fissure width more than 2 SD below the mean), moderate or severe CNS impairment (microcephaly and/or cognitive deficits more than 2 SD from mean in three or more domains), and confirmed prenatal alcohol exposure. Partial FAS (pFAS) is characterized by at least moderate facial abnormalities (one or more of: abnormally thin upper lip, abnormally smooth philtrum, or palpebral fissure width more than 2 SD below the mean), moderate or severe CNS impairment, and confirmed prenatal alcohol exposure. Growth deficiency is not required for pFAS. Static Encephalopathy is characterized by moderate or severe CNS impairment. Sentinel Physical Findings (dysmorphic facial features and growth deficiency) may or may not be present along with Static Encephalopathy. For pFAS, confirmed maternal alcohol consumption is required at either a "high risk" level (estimated >100 mg/dl blood alcohol

concentration weekly, early in pregnancy) or a lower level that is still associated with "some risk." For Static Encephalopathy / Sentinel Physical Findings, maternal alcohol exposure may be either confirmed as heavy (see examples below) or may be only suspected - but only when facial dysmorphology is also present.

Eighteen out of 21 participants with FASD had confirmed documentation of prenatal alcohol exposure (Astley and Clarren rank 3 or 4, corresponding to a diagnosis of FAS, pFAS, sentinel physical finding(s)/static encephalopathy, static encephalopathy or sentinel physical finding(s)/neurobehavioral disorder). Confirmed exposure included self-report by the biological parent or social service records indicating heavy maternal use during pregnancy. As an example, a rank of 4 was assigned if the mother's alcohol use was documented specifically as daily and chronic or consisting of weekly heavy binges during pregnancy. In contrast, rank 3 was assigned when heavy maternal alcohol consumption was documented but was neither daily nor were binge episodes weekly. Documentation of several heavy binge drinking episodes during pregnancy resulted in assigning a rank of 3. Potential participants were excluded if only minimal alcohol use was documented (for example, a single drink consumed on several occasions during pregnancy). In three cases, maternal alcohol use was suspected by a third party but was neither self-reported by the biological mother nor formally observed and documented by a third party. These 3 subjects were included because they had suspected exposure along with each of the three other criteria: growth deficiency (rank 3 or 4), facial dysmorphology (rank 2, 3, or 4), and evidence of cognitive dysfunction (3 or 4). Subjects with FASD were excluded for other prenatal drug exposure (except nicotine and

caffeine), although cocaine use by the mother was known in two cases. In four cases, there was suspected maternal marijuana use during pregnancy but no information about the extent of the use. In all four of these cases, alcohol was the predominant substance of abuse and alcohol use was reported to have been extensive during pregnancy.

Additional exclusion criteria for all subjects (FASD and controls) were the presence of another developmental disorder (ex. Autism, Down Syndrome), very low birthweight (<1500 grams), neurological disorder, traumatic brain injury, other medical condition affecting the brain, substance use in the participant themselves, or contraindications to safe MRI scanning. Control subjects were excluded for any parent-reported history of prenatal substance exposure, substance use in the participant themselves, and for history of psychiatric disorder or learning disability. We observed significant psychiatric co-morbidity in our participants with FASD, as has been extensively reported in the literature (O'Connor et al., 2002; Steinhausen et al., 1993; Streissguth et al., 2004; Streissguth and O'Malley, 2000). Participants with FASD were not excluded for psychiatric co-morbidity. The following co-morbid diagnoses were present in the group with FASD as established by full clinical evaluation: *Attention-Deficit / Hyperactivity Disorder* (76%); *Oppositional Defiant Disorder* (29%); *Post-Traumatic Stress Disorder* (24%); *Disruptive Behavior Disorder Not Otherwise Specified* (24%); *Reactive Attachment Disorder* (10%); *Developmental Communication Disorder* (10%); *Major Depressive Disorder* (5%); *Anxiety Disorder Not Otherwise Specified* (5%). Table 3 contains additional subject characteristics.

Table 3. Subject characteristics for FASD and control groups in Study #2.

N(%) or mean ± sd	FASD (n =21)	Control (n =23)	Statistical Test
Age at MRI scan	13.9 ± 2.3 yrs.	12.8 ± 2.4 yrs.	t=1.52, p=.14
Gender			
Male	12 (27%)	13 (30%)	
Female	9 (20%)	10 (23%)	χ^2=.002, p=.967
Handedness			
Right	20 (45%)	20(45%)	
Left	3 (7%)	1(3%)	χ^2=.911, p=.340
Facial Features (FASD only)			
(Astley & Clarren ratings)			
1. None	4 (19%)	-	-
2. Mild	4 (19%)	-	-
3. Moderate	5 (24%)	-	-
4. Severe	8 (38%)	-	-
Alcohol Exposure (FASD only)			
(Astley & Clarren ratings)			
1. No Risk	0 (0%)	-	-
2. Unknown Risk	3 (14%)	-	-
3. Some Risk	13 (62%)	-	-
4. High Risk	5 (24%)	-	-
FASD Category (Astley & Clarren)			
"Other FASD" including Sentinel Physical Findings & Static Encephalopathy	9 (43%)	-	-
Partial FAS	11 (52%)	-	-
FAS	1 (5%)	-	-
Intellectual Functioning			
Verbal Comprehension Index	88 ± 10.4	113 ± 12.7	t=7.25, p<.001
Perceptual Reasoning Index	93 ± 12.3	117 ± 12.6	t=6.40, p<.001
Working Memory Index	88 ±16.3	112 ± 11.7	t=5.73, p<.001
Processing Speed Index	86 ± 16.2	103 ± 13.2	t=3,88, p<.001

All procedures were approved by the University of Minnesota's Research Subjects' Protection Program and all participants underwent a comprehensive informed consent procedure. Participants were compensated with gift cards for their time.

Neuropsychological Evaluation

Participants were administered either the Wechsler Intelligence Scales for Children – Fourth Edition (WISC-IV) (Wechsler, 2003) (ages 10-16) or the Wechsler Adult Intelligence Scales – Third Edition (WAIS-III) (Wechsler, 1997) (age 17) by a

research assistant, psychometrist, or doctoral-level psychology trainee. Most of the participants with FASD were administered the test as part of their evaluation in the FASD Clinic. Control subjects were administered the IQ test at the time of the MRI.

MRI acquisition procedures

Subjects were scanned using a Siemens 3T TIM Trio MRI scanner with a 12-channel parallel array head coil. The imaging sequence and parameters for each scan are listed in Table 4. In all cases, the MRI scan was performed within one year of the IQ test. Participants were not sedated for the MRI scan nor were their usual medications modified for purposes of the MRI scan.

Table 4. MRI sequence and parameters.

Sequence	Imaging Parameters	Purpose	Time
Scout	3 plane localizer	Positioning	1 min
T1-weighted MPRAGE	TR=2350ms, TE=3.65ms, TI=1100ms, 224 slices, voxel size= 1x1x1mm, FOV=256mm, flip angle=7 degrees, GRAPPA 2.	Segmentation & cortical parcellation	5 min
Diffusion weighted (DTI)	TR=8500ms, TE=90ms, 64 slices, voxel size=2x2x2mm, FOV=256mm, GRAPPA 2, 30 volumes with b=1000 s/mm^2 & 6 with b=0 s/mm^2.	Computation of the diffusion tensor	6 min
DTI Field-map	Positioned to match DTI, 64 slices, voxel size=2x2x2mm, FOV=256mm TR=700ms, TE=4.62ms / 7.08ms, flip angle=90 deg.	Correction of geometric distortions for DTI	3 min
Resting fMRI	TR=2000 ms, TE=30ms, 34 interleaved slices, no skip, voxel size= 3.45x3.45x4.0mm, FOV=220mm, flip angle=77 deg., 180 measures.	Measurement of BOLD signal	6 min
fMRI Field map	Positioned to match fMRI, 34 slices, voxel size=3.45x3.45x4.0mm, FOV=220mm TR=700ms, TE=1.91ms / 3.37ms, flip angle=90 deg.	Correction for geometric distortions for fMRI	1 min

MRI post-processing

Several tools from the FMRIB's Software Library (FSL) version 4.0.1 were used in the post-processing (Smith et al., 2004; Woolrich et al., 2009).

T1 processing: Cortical reconstruction and segmentation were applied to the 1mm isotropic volume using FreeSurfer (Dale et al., 1999). Processing included removal of non-brain tissue, automated Talairach transformation, segmentation, intensity normalization, tessellation of the grey matter / white matter boundary, topology correction, surface deformation, and automated parcellation. FreeSurfer morphometric procedures have high test-retest reliability (Han et al., 2006). Each subject's data was visually inspected by a trained operator to ensure accuracy of the cortical parcellation. Hand editing was not employed. Cortical grey and white matter ROIs from FreeSurfer were aligned to both the fMRI and DTI data using a linear registration (FLIRT: FMRIB's Linear Image Registration Tool) (Jenkinson and Smith, 2001).

DTI processing: Eddy current distortion was corrected with FLIRT (Jenkinson and Smith, 2001). Geometric distortions caused by susceptibility-induced field inhomogeneities were corrected using the DTI field map data (FUGUE: FMRIB's Utility for Geometrically Unwarping EPIs) (Smith et al., 2004). The tensor was computed with FDT (FMRIB's Diffusion Toolbox) (Behrens et al., 2003). Mean Diffusivity (MD) (mean of the three eigenvalues), and Fractional Anisotropy (FA) were derived.

Resting fMRI processing: Brain extraction (BET) (Smith, 2002) and motion correction (MCFLIRT) (Jenkinson et al., 2002) were performed. Grand mean intensity normalization was applied. Geometric distortions caused by susceptibility-induced magnetic field inhomogeneities were corrected with FUGUE using the fMRI field map (Smith et al., 2004). These data were corrected for slice-timing, then a .01 to .08 Hz.

temporal bandpass filter was applied and the first three time points were dropped to allow for magnetization stabilization (FEAT: FMRIB's Expert Analysis Tool).

DTI tractography method: We applied a slightly modified version of the semi-automated corpus callosum tractography method that is described in detail in a previous paper (Wozniak et al., 2009). Briefly, an operator manually defined a rectangular mask outlining the corpus callosum and the border between the genu and the rostrum at the midline on the FMRIB58 FA map. The rectangular mask was warped into the native space of each subject and was then automatically partitioned into seven regions based on delineations from Witelson (1989). These rectangular regions were then segmented to fit the callosum using the x-component of the primary eigenvector. This analysis included the seventh region (rostrum) which was not included in the Wozniak et al. (2009) paper (Study #1). For the current analysis, FNIRT (FMRIB's Non-linear Image Registration Tool) was used instead of the FLIRT linear registration tool. The new analysis also used the FMRIB58 1mm isotropic FA map as a template instead of the MNI template brain that was used in Wozniak et al. (2009). The FMRIB brain was rotated to align it to the corpus callosum. The seven regions were then used as seed points for probabilistic tractography (FMRIB's Probtrack) of tracts projecting into right and left hemispheres. From anterior to posterior, the tracts were: 1. Rostrum; 2 Genu; 3. Rostral Body; 4. Anterior Mid-body; 5. Posterior Mid-body; 6. Isthmus; and 7. Splenium. Mean FA and MD were computed for each of these seven inter-hemispheric tracts. The reliability of this method is high, as described in Wozniak et al. (2009) (Study #1).

Functional connectivity method: A multimodal functional connectivity analysis was conducted with the following goals: 1. determine which bilateral cortical regions are interconnected by the seven inter-hemispheric tracts, 2. ascertain whether these interconnected regions exhibit altered functional connectivity. To accomplish goal 1, we first determined which bilateral cortical regions were at the distal ends of each of the corpus callosum tracts. FreeSurfer processing was performed on the T1-weighted images to parcellate the cortex into 35 cortical grey and associated white matter ROIs per hemisphere. The FreeSurfer parcellation was aligned to the FA map, overlap between each of the seven corpus callosum tracts and each right and left FreeSurfer white matter ROI was determined for every subject, and the overlap (percentage of voxels in common between each tract and FreeSurfer ROI) was averaged across the entire study population because there were not significant group differences in overlap. Using this method, four sets of cortical ROIs (right and left) were found to have the most significant overlap with the corpus callosum tracts: 1. Medial-orbitofrontal; 2. Superior-frontal; 3. Para-central; and 4. Pre-cuneus. Table 5 shows the relationship between corpus callosum tracts and FreeSurfer ROIs. Also included for reference are known fiber projections from the callosum based on anatomical studies (Aboitiz et al., 1992). Figure 5 illustrates the relationship between one set of cortical ROIs and the corresponding corpus callosum tract.

Table 5. Corpus callosum regions of interest (ROIs), corresponding cortical regions to which fibers project, and associated FreeSurfer grey matter ROIs at the distal ends of the white matter tracts.

Midline Corpus Callosum Region (Witelson, 1989)	Cortical region to which fibers project according to anatomical studies (Aboitz et al, 1992; Witelson, 1989)	FreeSurfer grey matter ROIs at the distal end of the white matter tracts (Dale et al., 1999)
1. Rostrum	*Caudal, orbital-prefrontal, & inferior pre-motor*	Medial Orbitofrontal
2. Genu	*Prefrontal*	Medial Orbitofrontal
3. Rostral Body	*Pre-motor and supplementary motor*	Superior Frontal
4. Anterior Mid-body	*Motor*	Superior Frontal
5. Posterior Mid-body	*Somasthetic and posterior parietal*	Para-Central
6. Isthmus	*Superior temporal and posterior parietal*	Para-Central
7. Splenium	*Occipital and inferior temporal*	Pre-Cuneus

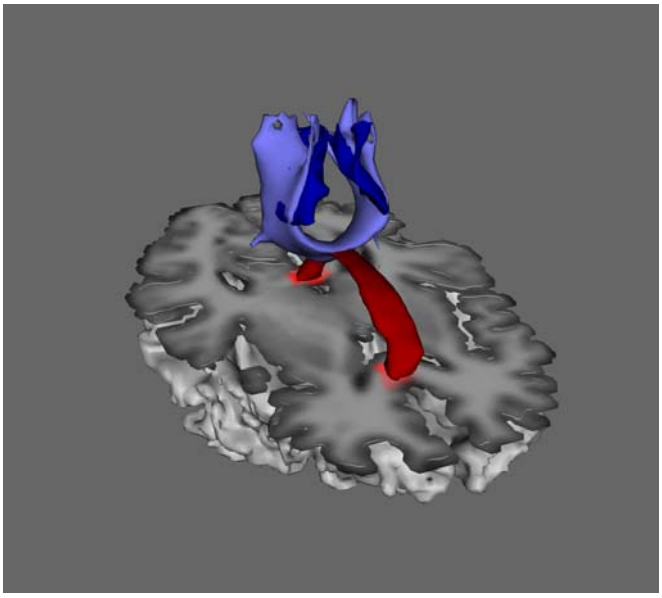

Figure 5. Illustration of the relationship between the isthmus corpus callosum tract (light blue) and the corresponding set of para-central cortical regions of interest (dark blue). Mean FA and MD were computed from all voxels in the corpus callosum tract (light blue). Mean BOLD time series were computed from all voxels in the cortical regions of interest (dark blue). The corpus callosum at the midline is included (red) for spatial reference.

To accomplish goal 2, the four sets of cortical ROIs identified above were probed for connectivity deficits by investigating functional connectivity in the resting-state fMRI data. These four cortical regions were aligned to the fMRI data using FLIRT with a linear six degree of freedom registration. Mean pixel intensity was computed within each

of the ROIs, yielding one value for each ROI at every time point. Separately, mean pixel intensity across the brain was also computed at every time point. A representative white matter time series was also extracted by applying an eroded mask comprising the Freesurfer right and left white matter ROIs to the fMRI data. Similarly, a representative cerebrospinal fluid (CSF) time series was extracted by applying a mask comprising the Freesurfer right and left lateral ventricle ROIs to the fMRI data. Custom MATLAB code was used to regress the four ROI time series against the six motion correction parameters, the whole brain voxel intensity time series, the white matter time series, and the CSF time series. Pearson product-moment time series correlations were computed for each of the four sets of right and left ROIs for each subject. Figure 6 illustrates time series from medial orbitofrontal ROIs with an example of high correlation in a control subject and low correlation in a subject with FASD.

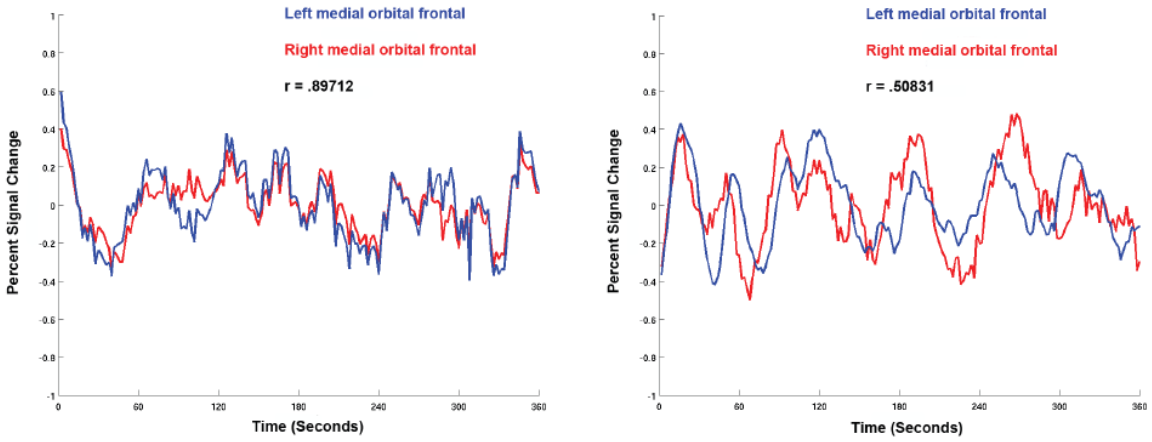

Figure 6. Sample six-minute resting fMRI time-series from two participants recorded from left (black) and right (gray) medial orbital-frontal regions of interest. The figure on the left, from a control subject, shows tight inter-hemispheric correlation. In contrast, the figure on the right, from a subject with FASD, shows much lower inter-hemispheric correlation.

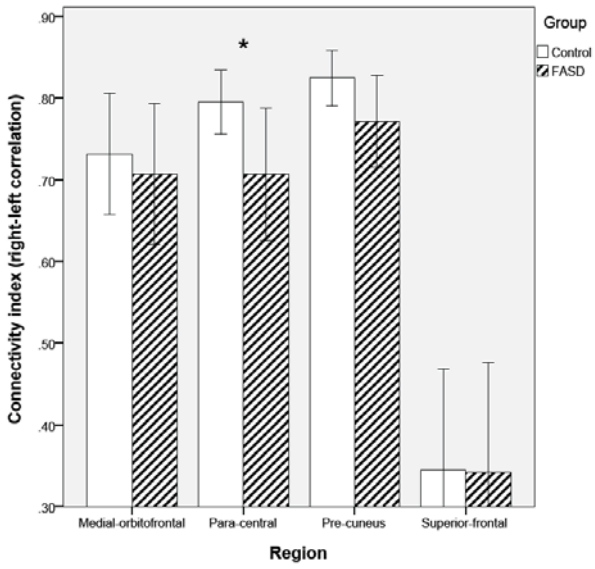

Figure 7. Inter-hemispheric connectivity by group (control vs. FASD) for four cortical regions of interest. A significant difference was observed in the para-central region (p<.01).**

RESULTS

Group comparison of motion during MRI scans

In addition to correcting the data for motion as detailed above, a group comparison was performed to test for any potential remaining systematic group difference in motion. The resting fMRI data were used for this comparison because of their relative sensitivity to motion. Translational motion (in mm.) and rotational motion (in radians) were used for these analyses (Liao et al., 2010; Liu et al., 2008). Independent samples t-tests showed that there were not significant group differences in the amount of translation [T=.434, p = .667] or rotation [T=.-.012, p = .991]. Therefore, motion was not entered as a covariate in any of the remaining statistical analyses.

Group differences in functional connectivity

Although the groups were matched on age and sex, the effects of these two subject factors on the dependent measures were tested nonetheless with general linear modeling. Neither was a significant factor and, thus, both were removed from further analyses. A MANOVA testing for differences between controls and FASD for the four inter-hemispheric functional connectivity measures was significant, Wilks' Lambda = .783, $F(4, 38) = 2.63$, $p = .049$ (the volume of the Freesurfer CSF ROI was included as a covariate in this analysis because we observed significant variability across subjects). As shown in Figure 4, connectivity was numerically lower for FASD vs. Controls in all four sets of ROIs, and univariate tests revealed a significant difference in the para-central ROIs, $F(1,43)=4.47$, $p =.041$. Children with FASD had inter-hemispheric para-central correlations that were 12.7% lower than controls.

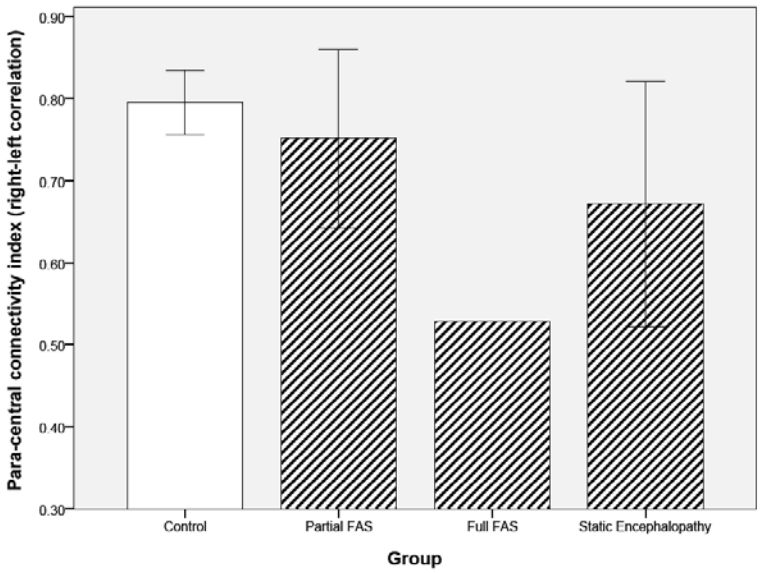

Figure 8. Inter-hemispheric connectivity in the para-central region by diagnostic group.

Unfortunately, the diagnostic sub-groups were not large enough to analyze for statistical differences in para-central connectivity, but an examination of the data is informative nonetheless. Figure 5 is noteworthy in that it shows the extremely tight variability of this connectivity measure in healthy control subjects in contrast to the wide variability among children with FASD. The low functional connectivity in the one subject with full FAS was expected and it supports the clinical relevance of the measure to some extent. The notably low level of functional connectivity in those with static encephalopathy is intriguing because this group is generally considered to be less severely affected.

Association with facial dysmorphology

Functional connectivity in the para-central ROIs was not found to be associated with facial dysmorphology as defined by 1-4 rankings from the Astley and Clarren diagnostic system. The Spearman correlation was .095, $p = .681$.

Functional / structural connectivity relationships

We next examined the relationship between inter-hemispheric functional connectivity of the para-central ROIs and microstructural integrity in the corresponding two corpus callosum tracts (isthmus and posterior mid-body) using one-tailed Pearson correlations. As hypothesized, low inter-hemispheric functional connectivity (low right-left correlation) in the para-central ROIs was associated at a trend level with increased MD in the isthmus tract (across all subjects: $r = -.23$, $p = .067$) (Controls: $r = -.30$, $p =$

.086; FASD: r = -.13, p = .383) and significantly in the posterior mid-body tract (all subjects: r = -.29, p = .026) (Controls: r = -.48, p = .01; FASD: r = -.19, p = .20). The correlations with FA were not significant in the isthmus (all subjects: r = .09, p = .287) (Controls: r = -.01, p = .493; FASD: r = .05, p = .419) nor the posterior mid-body (all subjects: r = .111, p = .238) (Controls: r = .292, p = .09; FASD: r = -.01, p = .485). To illustrate the relative specificity of the association between para-central functional connectivity and MD in posterior corpus callosum tracts, Table 4 lists all of the correlation coefficients between para-central ROI functional connectivity and MD in the callosal tracts in positional order from anterior to posterior. The data show a general pattern of stronger association with posterior callosal MD compared with anterior callosal MD, peaking in the posterior-midbody, isthmus, and splenium regions. Breaking this analysis down by groups reveals that this pattern is especially evident in the controls, but that the relationship is less evident in the FASD group alone.

Inter-hemispheric connectivity and cognitive functioning

A series of four linear regression analyses were conducted to examine the relative contributions of structural and functional connectivity measures in explaining variance in cognitive functioning. The index scores from the Wechsler intelligence test (WISC-IV or WAIS-III) served as the dependent measures for these analyses. Predictor variables for each regression were the para-central connectivity measure and mean diffusivity from the two associated corpus callosum tracts (isthmus and posterior mid-body). For the Verbal Comprehension Index (VCI), the regression was non-significant, $R^2 = .098$, $F(3, 43) =$

1.44, p = .245. For the Perceptual Reasoning Index (PRI), the regression was at a trend level, R^2 = .146, F(3,43) = 2.28, p = .095. Beta coefficients were as follows: para-central connectivity = .083, t = .553, p = .583, isthmus mean diffusivity = -.440, t = -2.13, p = .039, and posterior mid-body mean diffusivity = .505, t = 2.47, p = .018. Two follow-up regressions by group (control and FASD) were not significant, likely due to the small sample size. For the Working Memory Index (WMI), the regression was non-significant, R^2 = -.010, F(3,43) = .865, p = .467. Lastly, for the Processing Speed Index (PSI), the regression was non-significant, R^2 = -.065, F(3,43) = .126, p = .944. In this set of analyses, perceptual reasoning was the cognitive factor most related to inter-hemispheric connectivity and it appears that the structural connectivity measures were stronger predictors than the functional connectivity measure in this case.

DISCUSSION

For the first time, we report disturbances in inter-hemispheric functional connectivity during a resting state in children with FASD using fMRI. For this first study, we focused on examining inter-hemispheric functional connectivity because our previous DTI work has clearly demonstrated underlying abnormalities in the microstructure of posterior corpus callosum fibers connecting the hemispheres (Wozniak et al., 2006; Wozniak et al., 2009). Those findings were consistent with numerous other studies showing abnormalities in corpus callosum structure, especially in the posterior regions (Bookstein et al., 2007; Fryer et al., 2009; Lebel et al., 2008; Li et al., 2009; Ma et al., 2005; Sowell et al., 2008; Sowell et al., 2001a).

Interestingly, the para-central region is one of eight anatomical sub-regions that Hagmann et al. (2008) identified as members of a "structural core" – regions that show elevated fiber counts / fiber densities and regions that had exceptionally high inter-hemispheric connectivity in their network analyses of diffusion spectrum imaging (DSI) tractography-based structural data. The other regions in the structural core include the posterior cingulate, precuneus, cuneus, the isthmus of the cingulate, superior temporal banks, and inferior and superior parietal cortex. Hagmann et al. (2008) characterize this structural core of medial posterior cortical regions as an integrated system that is critical to the coordination of the two hemispheres. This characterization points out the potentially devastating cognitive effects of the structural and functional connectivity abnormalities in these regions that we have now described in FASD.

In the current study, we did not observe a significant relationship between inter-hemispheric functional connectivity in the para-central region and facial dysmorphology. This analysis is somewhat limited by the inclusion of only one participant with full FAS, but there was a range of facial dysmorphology in the sample. In general, this is consistent with our previous studies which did not show a relationship between microstructural integrity of the callosum and facial dysmorphology (Wozniak et al., 2006; Wozniak et al., 2009) and with the view that brain damage and facial stigmata may be semi-independent outcomes of prenatal alcohol exposure (Bookstein et al., 2002a; Connor et al., 2006). A number of other studies have failed to find relationships between facial characteristics and callosal measures. For example, Bookstein et al. (2007; 2002b) found no evidence of a relationship between callosal shape abnormalities and facial

dysmorphology. The lack of a relationship between brain and face abnormalities is not inconsistent with the general consensus in the literature that facial dysmorphology is only present in a subset of individuals affected by prenatal alcohol exposure (Stratton et al., 1996) and is tied to a specific window of exposure to alcohol (Sulik, 2005), whereas brain damage may be an outcome of alcohol exposure across a much wider window of exposure during gestation.

The clinical relevance of corpus callosum abnormalities in FASD has been shown in a number of studies that demonstrate associations with cognitive deficits. The current finding of a trend-level relationship between Wechsler Perceptual Reasoning Index score and connectivity mediated via the posterior callosum is consistent with our previous report of a significant association between posterior callosal mean diffusivity and performance on the Wechsler PRI ($r = -.45$, $p = .008$) (Wozniak et al., 2009). Similarly, Sowell et al. (2008) showed that fractional anisotropy in the splenium of the corpus callosum was correlated with visuomotor integration skill in children with FASD. Pfefferbaum and colleagues (2006) have observed similar regionally-specific relationships between visuospatial functioning and posterior callosum integrity in alcoholism and have hypothesized that certain tasks requiring bilateral integration are particularly affected by the relatively subtle callosal abnormalities that are seen with DTI. In FASD, corpus callosum shape abnormalities are also known to be associated with executive functioning (Bookstein et al., 2002b) and verbal memory (Sowell et al., 2001a). The current data suggest that DTI microstructural connectivity measures in the posterior callosum may be better predictors of perceptual reasoning ability than the fMRI

functional connectivity measure used here. Future studies with larger samples will be able to examine the relative contributions of structural and functional connectivity measures in more depth.

A few studies have focused on the contribution of corpus callosum integrity to inter-hemispheric transfer in FASD. Roebuck et al. (2002) provided evidence that children with FASD have less than optimal inter-hemispheric transfer as evidenced by their performance on the "crossed" condition of a finger localization task. Furthermore, they demonstrated associations between poor task performance and reduced corpus callosum volumes in both anterior and posterior regions. Dodge et al. (2009) also used a finger localization task to examine inter-hemispheric transfer in FASD. They found that children with FASD made more errors on the task and that errors were associated with volume reductions in the isthmus and splenium regions of the corpus callosum. DTI studies suggest that inter-hemispheric transfer is related to even more subtle measures of microstructural corpus callosum integrity. In a sample of healthy, normally-developing children and young adults, Muetzel et al. (2008) showed that FA in the splenium was associated with alternating hand performance on a finger tapping task. A functional/structural connectivity relationship has also been shown using EEG coherence and corpus callosum DTI measures in healthy adults (Teipel et al., 2009). In that study, right-left EEG coherence in the temporal-parietal region was correlated with fractional anisotropy in posterior white matter including posterior corpus callosum. In general, inter-hemispheric transfer of information other than sensory-motor information is challenging to study. For the current study, we utilized a non-task based approach to

examine inter-hemispheric functional connectivity, mediated by corpus callosum, during a resting state. In this manner, our functional connectivity measures served as proxy measures of inter-hemispheric transfer of information. The non-task based approach to functional connectivity may have some advantages over task-based approaches in that it may be applicable to younger participants and/or significantly impaired participants who might have difficulty performing tasks.

Limitations to the interpretation of the current results are acknowledged. First, we observed significant psychiatric co-morbidity in the participants with FASD and intentionally did not exclude for co-morbidity. Eliminating potential participants with co-existing psychiatric diagnoses would have significantly limited enrollment in the study and, more importantly, would have seriously limited the generalizability of the results. FASD is well-known to be associated with significant psychiatric co-morbidity of the type that we observed (O'Connor et al., 2002; Steinhausen et al., 1993; Streissguth et al., 2004; Streissguth and O'Malley, 2000). Because Fetal Alcohol spectrum Disorders themselves and the associated psychiatric co-morbidity are both likely related to the underlying neurodevelopmental effects of alcohol, it will likely be extremely difficult to entirely separate the two completely. However, future studies might begin to parse out the effects of these co-morbid disorders by including comparison groups for the major co-morbidities including Attention-Deficit Hyperactivity Disorder and Oppositional Defiant Disorder. A second potential limitation of the study relates to the diagnostic system used (Astley and Clarren's 4-Digit code), for which there is not universal agreement. Alternate diagnostic criteria exist, including those proposed by the Institute

of Medicine (1996) and modified by Hoyme et al. (2005) as well as those proposed by the Centers for Disease Control and Prevention for FAS (Bertrand et al., 2004). Critics of the 4-Digit coding system have argued that it is overly complex, it over-emphasizes brain dysfunction (which is a non-specific component of the syndrome), it is subject to problems with diagnostic consensus, and may over-diagnose FASD (Benz et al., 2009; Hoyme et al., 2005; Jones et al., 2006). The current study attempted to address some of these concerns by only enrolling participants with confirmed heavy alcohol exposure and/or measurable facial dysmorphology in addition to cognitive dysfunction. A more narrow focus on full FAS could have been taken, but would have limited the generalizability of the results.

Thus far, this is the first study to examine inter-hemispheric functional connectivity in FASD. The data suggest that communication between homologous cortical regions is disturbed in FASD, and is specifically disturbed in those regions connected by posterior corpus callosum fibers, especially the isthmus and splenium. Because this disturbance in functional connectivity may be related to macrostructural or microstructural abnormalities and to cognitive functioning, further efforts to examine functional connectivity in FASD are warranted. The current analyses suggested that the relationship between regional microstructural connectivity and functional connectivity is stronger in non-exposed controls versus children with FASD. At this point, it is unclear why this would be the case. One possibility is that greater variability in white matter anatomy at the macroscopic level among those with FASD may be adding variability to these analyses of microstructural integrity. Small sample size may also have been a

factor. Thus, future studies with larger numbers of subjects may benefit from additional analyses of potential differences in anatomy such as differences in white matter fiber projections as determined by DTI tractography.

Overall the connectivity methods used here can easily be extended to other white matter tracts in the brain, allowing for examination of additional networks. A number of analysis approaches have been described (Fox and Raichle, 2007) and are potentially applicable to FASD including placing multiple seeds in known anatomical networks (Kelly et al., 2009; Margulies et al., 2007) or applying independent components analysis in a purely empirical derivation of functional networks (Beckmann et al., 2005; Biswal et al., 2003; Greicius et al., 2004).

In addition to providing data that complement the findings of white matter structural abnormalities in FASD, these types of functional connectivity measures may serve an additional role in providing quantitative metrics of brain health. In turn, these metrics may be useful in exploring subgroups of individuals with FASD, further examining relationships with cognitive functioning, and possibly evaluating the effects of new interventions for neurodevelopmental conditions including FASD. Recent interventions targeting early neurodevelopment in those exposed to alcohol, such as peri-natal nutritional supplementation, will ultimately be evaluated by sensitive measures of brain status such as microstructural integrity and functional connectivity. Although abnormalities in these characteristics are not likely to be specific to FASD and there will be challenges to interpreting the data in light of findings in common co-morbid conditions such as ADHD (Konrad and Eickhoff, 2010), it is possible that these measures

may prove to be uniquely sensitive to the effects of prenatal alcohol exposure and, thus, useful in further understanding the full range of effects across the full FASD spectrum.

CONCLUSION

The existing DTI data show evidence of microstructural white matter abnormalities in individuals who were exposed prenatally to alcohol. The precise pathology underlying these neuroimaging abnormalities is not yet known, but could be related to one or more characteristics of white matter organization including axonal size, density, packing, water content, and myelination. Because these abnormalities appear to be related to cognitive functioning, they may be critical in understanding the origins of the common deficits seen in FASD, including visual-perceptual abnormalities, attention and executive functioning deficits, and behavioral and emotional dysregulation. The fact that these particular brain abnormalities are not correlated with dysmorphic facial features in FASD suggests that these two characteristics may provide independent information about the effects of exposure on the individual. This independence also highlights the potential limitations of facial characteristics in terms of their sensitivity to the underlying syndrome and limitations in their capacity as measures of syndrome severity.

DTI has provided us with a unique window into the fine details of *structural connectivity* in the brain – during development and also following insults to the developmental process such as those resulting from prenatal alcohol exposure. The next logical step, which has been introduced here in Study #2, is to incorporate measures of

functional connectivity into future investigations. The examination of these types of networks using resting-state fMRI is thought to provide a measure of "intrinsic" brain activity – brain activity that is distinct from the brain response that occurs to extrinsic stimuli, such as during a task-based fMRI study. Brain activity during the resting state may reflect ongoing integration of information, consolidation of memories, maintenance of salient connections, and even preparation for action. The patterns of functional connectivity that are seen during rest are also a reflection of the underlying structural connectivity in the brain.

These functional connectivity methods will likely prove very relevant to the study of developmental disorders including FASD. Future studies of FASD will be able to examine whole brain connectivity in greater detail, combining structural connectivity measures from DTI with functional connectivity measures from resting-state fMRI to better characterize the extent of the abnormalities in this population.

BIBLIOGRAPHY

Abel, E. L. (1995). An update on incidence of FAS: FAS is not an equal opportunity birth defect. *Neurotoxicol Teratol, 17*(4), 437-443.

Aboitiz, F., Scheibel, A. B., Fisher, R. S., & Zaidel, E. (1992). Fiber composition of the human corpus callosum. *Brain Res, 598*(1-2), 143-153.

Alexander, A. L., Lee, J. E., Lazar, M., Boudos, R., DuBray, M. B., Oakes, T. R., et al. (2007). Diffusion tensor imaging of the corpus callosum in Autism. *Neuroimage, 34*(1), 61-73.

Alkonyi, B., Govindan, R. M., Chugani, H. T., Behen, M. E., Jeong, J. W., & Juhasz, C. (2010). Focal white matter abnormalities related to neurocognitive dysfunction: An objective diffusion tensor imaging study of children with Sturge-Weber syndrome. *Pediatric Research*.

Archibald, S. L., Fennema-Notestine, C., Gamst, A., Riley, E. P., Mattson, S. N., & Jernigan, T. L. (2001). Brain dysmorphology in individuals with severe prenatal alcohol exposure. *Dev Med Child Neurol, 43*(3), 148-154.

Ashtari, M., Kumra, S., Bhaskar, S. L., Clarke, T., Thaden, E., Cervellione, K. L., et al. (2005). Attention-deficit/hyperactivity disorder: a preliminary diffusion tensor imaging study. *Biol Psychiatry, 57*(5), 448-455.

Barkovich, A. J., Kjos, B. O., Jackson, D. E., Jr., & Norman, D. (1988). Normal maturation of the neonatal and infant brain: MR imaging at 1.5 T. *Radiology, 166*(1 Pt 1), 173-180.

Barnea-Goraly, N., Kwon, H., Menon, V., Eliez, S., Lotspeich, L., & Reiss, A. L. (2004). White matter structure in autism: preliminary evidence from diffusion tensor imaging. *Biological Psychiatry, 55*(3), 323-326.

Barnea-Goraly, N., Menon, V., Eckert, M., Tamm, L., Bammer, R., Karchemskiy, A., et al. (2005). White matter development during childhood and adolescence: a cross-sectional diffusion tensor imaging study. *Cereb Cortex, 15*(12), 1848-1854.

Basser, P. J. (1995). Inferring microstructural features and the physiological state of tissues from diffusion-weighted images. *NMR Biomed, 8*(7-8), 333-344.

Basser, P. J., Mattiello, J., & LeBihan, D. (1994a). Estimation of the effective self-diffusion tensor from the NMR spin echo. *J Magn Reson B, 103*(3), 247-254.

Basser, P. J., Mattiello, J., & LeBihan, D. (1994b). MR diffusion tensor spectroscopy and imaging. *Biophys J, 66*(1), 259-267.

Basser, P. J., & Pierpaoli, C. (1996). Microstructural and physiological features of tissues elucidated by quantitative-diffusion-tensor MRI. *Journal of Magnetic Resonance. Series B, 111*(3), 209-219.

Basser, P. J., & Pierpaoli, C. (1998). A simplified method to measure the diffusion tensor from seven MR images. *Magn Reson Med, 39*(6), 928-934.

Beaulieu, C. (2002). The basis of anisotropic water diffusion in the nervous system - a technical review. *NMR Biomed, 15*(7-8), 435-455.

Beaulieu, C. (2009). The biological basis of diffusion anisotropy. In H. B. Johansen-Berg, E.J. (Ed.), *From quantitative measurement to in-vivo neuroanatomy*. London, UK: Academic Press.

Bhatara, V., Loudenberg, R., & Ellis, R. (2006). Association of attention deficit hyperactivity disorder and gestational alcohol exposure: an exploratory study. *J Atten Disord, 9*(3), 515-522.

Biswal, B., Yetkin, F. Z., Haughton, V. M., & Hyde, J. S. (1995). Functional connectivity in the motor cortex of resting human brain using echo-planar MRI. *Magn Reson Med, 34*(4), 537-541.

Bonekamp, D., Nagae, L. M., Degaonkar, M., Matson, M., Abdalla, W. M., Barker, P. B., et al. (2007). Diffusion tensor imaging in children and adolescents: reproducibility, hemispheric, and age-related differences. *Neuroimage, 34*(2), 733-742.

Bookstein, F. L., Sampson, P. D., Connor, P. D., & Streissguth, A. P. (2002). Midline corpus callosum is a neuroanatomical focus of fetal alcohol damage. *Anat Rec, 269*(3), 162-174.

Bookstein, F. L., Sampson, P. D., Streissguth, A. P., & Connor, P. D. (2001). Geometric morphometrics of corpus callosum and subcortical structures in the fetal-alcohol-affected brain. *Teratology, 64*(1), 4-32.

Bookstein, F. L., Streissguth, A. P., Sampson, P. D., Connor, P. D., & Barr, H. M. (2002). Corpus callosum shape and neuropsychological deficits in adult males with heavy fetal alcohol exposure. *Neuroimage, 15*(1), 233-251.

Broyd, S. J., Demanuele, C., Debener, S., Helps, S. K., James, C. J., & Sonuga-Barke, E. J. (2008). Default-mode brain dysfunction in mental disorders: A systematic review. *Neurosci Biobehav Rev, 33*(3), 279-296.

Cao, Q., Sun, L., Gong, G., Lv, Y., Cao, X., Shuai, L., et al. (2010). The macrostructural and microstructural abnormalities of corpus callosum in children with attention deficit/hyperactivity disorder: a combined morphometric and diffusion tensor MRI study. *Brain Res, 1310*, 172-180.

Chanraud, S., Zahr, N., Sullivan, E. V., & Pfefferbaum, A. (2010). MR diffusion tensor imaging: a window into white matter integrity of the working brain. *Neuropsychology Review, 20*(2), 209-225.

Cloak, C. C., Ernst, T., Fujii, L., Hedemark, B., & Chang, L. (2009). Lower diffusion in white matter of children with prenatal methamphetamine exposure. *Neurology, 72*(24), 2068-2075.

Cykowski, M. D., Fox, P. T., Ingham, R. J., Ingham, J. C., & Robin, D. A. (2010). A study of the reproducibility and etiology of diffusion anisotropy differences in developmental stuttering: a potential role for impaired myelination. *Neuroimage, 52*(4), 1495-1504.

Davenport, N. D., Karatekin, C., White, T., & Lim, K. O. (2010). Differential fractional anisotropy abnormalities in adolescents with ADHD or schizophrenia. *Psychiatry Res, 181*(3), 193-198.

Della Grotta, S., LaGasse, L. L., Arria, A. M., Derauf, C., Grant, P., Smith, L. M., et al. (2010). Patterns of methamphetamine use during pregnancy: results from the Infant Development, Environment, and Lifestyle (IDEAL) Study. *Matern Child Health J, 14*(4), 519-527.

Eluvathingal, T. J., Hasan, K. M., Kramer, L., Fletcher, J. M., & Ewing-Cobbs, L. (2007). Quantitative diffusion tensor tractography of association and projection fibers in normally developing children and adolescents. *Cereb Cortex, 17*(12), 2760-2768.

Fair, D. A., Cohen, A. L., Dosenbach, N. U., Church, J. A., Miezin, F. M., Barch, D. M., et al. (2008). The maturing architecture of the brain's default network. *Proc Natl Acad Sci U S A, 105*(10), 4028-4032.

Faria, A. V., Hoon, A., Stashinko, E., Li, X., Jiang, H., Mashayekh, A., et al. (2010). Quantitative analysis of brain pathology based on MRI and brain atlases-Applications for cerebral palsy. *Neuroimage*.

Filippi, C. G., Lin, D. D., Tsiouris, A. J., Watts, R., Packard, A. M., Heier, L. A., et al. (2003). Diffusion-tensor MR imaging in children with developmental delay: preliminary findings. *Radiology, 229*(1), 44-50.

Filley, C. M. (1998). The behavioral neurology of cerebral white matter. *Neurology, 50*(6), 1535-1540.

Filley, C. M., & Kleinschmidt-DeMasters, B. K. (2001). Toxic leukoencephalopathy. *N Engl J Med, 345*(6), 425-432.

Fox, R. J., Cronin, T., Lin, J., Wang, X., Sakaie, K., Ontaneda, D., et al. (2010). Measuring Myelin Repair and Axonal Loss with Diffusion Tensor Imaging. *AJNR. American Journal of Neuroradiology*.

Fryer, S. L., McGee, C. L., Matt, G. E., Riley, E. P., & Mattson, S. N. (2007). Evaluation of psychopathological conditions in children with heavy prenatal alcohol exposure. *Pediatrics, 119*(3), e733-741.

Fryer, S. L., Schweinsburg, B. C., Bjorkquist, O. A., Frank, L. R., Mattson, S. N., Spadoni, A. D., et al. (2009). Characterization of White Matter Microstructure in Fetal Alcohol Spectrum Disorders. *Alcohol Clin Exp Res, 33*(3), 1-8.

Gao, W., Lin, W., Chen, Y., Gerig, G., Smith, J. K., Jewells, V., et al. (2008). Temporal and Spatial Development of Axonal Maturation and Myelination of White Matter in the Developing Brain. *AJNR Am J Neuroradiol, 30*(2), 290-296.

Geschwind, N. (1965). Disconnexion syndromes in animals and man. I. *Brain, 88*(2), 237-294.

Giorgio, A., Watkins, K. E., Chadwick, M., James, S., Winmill, L., Douaud, G., et al. (2009). Longitudinal changes in grey and white matter during adolescence. *Neuroimage*.

Giorgio, A., Watkins, K. E., Chadwick, M., James, S., Winmill, L., Douaud, G., et al. (2010). Longitudinal changes in grey and white matter during adolescence. *Neuroimage, 49*(1), 94-103.

Giorgio, A., Watkins, K. E., Douaud, G., James, A. C., James, S., De Stefano, N., et al. (2008). Changes in white matter microstructure during adolescence. *Neuroimage, 39*(1), 52-61.

Greicius, M. (2008). Resting-state functional connectivity in neuropsychiatric disorders. *Curr Opin Neurol, 21*(4), 424-430.

Groen, W. B., Buitelaar, J. K., van der Gaag, R. J., & Zwiers, M. P. (2010). Pervasive microstructural abnormalities in autism: a DTI study. *Journal of Psychiatry and Neuroscience*.

Hamilton, L. S., Levitt, J. G., O'Neill, J., Alger, J. R., Luders, E., Phillips, O. R., et al. (2008). Reduced white matter integrity in attention-deficit hyperactivity disorder. *Neuroreport, 19*(17), 1705-1708.

Hasan, K. M., Kamali, A., Iftikhar, A., Kramer, L. A., Papanicolaou, A. C., Fletcher, J. M., et al. (2009). Diffusion tensor tractography quantification of the human corpus callosum fiber pathways across the lifespan. *Brain Res, 1249*, 91-100.

Hasan, K. M., Kamali, A., Kramer, L. A., Papnicolaou, A. C., Fletcher, J. M., & Ewing-Cobbs, L. (2008). Diffusion tensor quantification of the human midsagittal corpus callosum subdivisions across the lifespan. *Brain Res, 1227*, 52-67.

Hayakawa, K., Konishi, Y., Kuriyama, M., Konishi, K., & Matsuda, T. (1991). Normal brain maturation in MRI. *Eur J Radiol, 12*(3), 208-215.

Hermoye, L., Saint-Martin, C., Cosnard, G., Lee, S. K., Kim, J., Nassogne, M. C., et al. (2006). Pediatric diffusion tensor imaging: normal database and observation of the white matter maturation in early childhood. *Neuroimage, 29*(2), 493-504.

Holland, B. A., Haas, D. K., Norman, D., Brant-Zawadzki, M., & Newton, T. H. (1986). MRI of normal brain maturation. *AJNR Am J Neuroradiol, 7*(2), 201-208.

Huang, H., Zhang, J., Wakana, S., Zhang, W., Ren, T., Richards, L. J., et al. (2006). White and gray matter development in human fetal, newborn and pediatric brains. *Neuroimage, 33*(1), 27-38.

Innocenti, G. M. (1986). General ogranization of callosal connections in cerebral cortex. In E. G. Jones (Ed.), *Cerebral Cortex* (pp. 291-354). New York: Plenum.

Jacobsen, L. K., Picciotto, M. R., Heath, C. J., Frost, S. J., Tsou, K. A., Dwan, R. A., et al. (2007). Prenatal and adolescent exposure to tobacco smoke modulates the development of white matter microstructure. *J Neurosci, 27*(49), 13491-13498.

Johnston, J. M., Vaishnavi, S. N., Smyth, M. D., Zhang, D., He, B. J., Zempel, J. M., et al. (2008). Loss of resting interhemispheric functional connectivity after complete section of the corpus callosum. *J Neurosci, 28*(25), 6453-6458.

Jones, D. K., & Cercignani, M. (2010). Twenty-five pitfalls in the analysis of diffusion MRI data. *NMR in Biomedicine, 23*(7), 803-820.

Kao, Y. C., Peng, S. S., Weng, W. C., Lin, M. I., & Lee, W. T. (2010). Evaluation of White Matter Changes in Agyria-Pachygyria Complex Using Diffusion Tensor Imaging. *Journal of Child Neurology*.

Keller, T. A., & Just, M. A. (2009). Altering cortical connectivity: remediation-induced changes in the white matter of poor readers. *Neuron, 64*(5), 624-631.

Kinney, H. C., Brody, B. A., Kloman, A. S., & Gilles, F. H. (1988). Sequence of central nervous system myelination in human infancy. II. Patterns of myelination in autopsied infants. *J Neuropathol Exp Neurol, 47*(3), 217-234.

Kobel, M., Bechtel, N., Specht, K., Klarhofer, M., Weber, P., Scheffler, K., et al. (2010). Structural and functional imaging approaches in attention deficit/hyperactivity disorder: does the temporal lobe play a key role? *Psychiatry Res, 183*(3), 230-236.

Kumar, M., Srivastava, A., Agarwal, S., Behari, S., Malik, G. K., Rathore, R. K., et al. (2010). Cognitive functions correlate with diffusion tensor imaging metrics in patients with spina bifida cystica. *Childs Nervous System*.

Le Bihan, D. (1995). Molecular diffusion, tissue microdynamics and microstructure. *NMR Biomed, 8*(7-8), 375-386.

Le Bihan, D. (2003). Looking into the functional architecture of the brain with diffusion MRI. *Nat Rev Neurosci, 4*(6), 469-480.

Lebel, C., Rasmussen, C., Wyper, K., Andrew, G., & Beaulieu, C. (2010). Brain microstructure is related to math ability in children with fetal alcohol spectrum disorder. *Alcoholism, Clinical and Experimental Research, 34*(2), 354-363.

Lebel, C., Rasmussen, C., Wyper, K., Walker, L., Andrew, G., Yager, J., et al. (2008). Brain diffusion abnormalities in children with fetal alcohol spectrum disorder. *Alcoholism: Clinical and Experimental Research, 23*(10), 1732-1740.

Lebel, C., Walker, L., Leemans, A., Phillips, L., & Beaulieu, C. (2008). Microstructural maturation of the human brain from childhood to adulthood. *Neuroimage, 40*(3), 1044-1055.

Li, L., Coles, C. D., Lynch, M. E., & Hu, X. (2009). Voxelwise and skeleton-based region of interest analysis of fetal alcohol syndrome and fetal alcohol spectrum disorders in young adults. *Hum Brain Mapp, 30*(10), 3265-3274.

Ma, X., Coles, C. D., Lynch, M. E., Laconte, S. M., Zurkiya, O., Wang, D., et al. (2005). Evaluation of corpus callosum anisotropy in young adults with fetal alcohol syndrome according to diffusion tensor imaging. *Alcohol Clin Exp Res, 29*(7), 1214-1222.

Masutani, Y., Aoki, S., Abe, O., Hayashi, N., & Otomo, K. (2003). MR diffusion tensor imaging: recent advance and new techniques for diffusion tensor visualization. *Eur J Radiol, 46*(1), 53-66.

Mattson, S. N., & Riley, E. P. (1998). A review of the neurobehavioral deficits in children with fetal alcohol syndrome or prenatal exposure to alcohol. *Alcohol Clin Exp Res, 22*(2), 279-294.

Mori, S., & Zhang, J. (2006). Principles of diffusion tensor imaging and its applications to basic neuroscience research. *Neuron, 51*(5), 527-539.

Moseley, M. E., Cohen, Y., Kucharczyk, J., Mintorovitch, J., Asgari, H. S., Wendland, M. F., et al. (1990). Diffusion-weighted MR imaging of anisotropic water diffusion in cat central nervous system. *Radiology, 176*(2), 439-445.

Muetzel, R. L., Collins, P. F., Mueller, B. A., A, M. S., Lim, K. O., & Luciana, M. (2008). The development of corpus callosum microstructure and associations with bimanual task performance in healthy adolescents. *Neuroimage, 39*(4), 1918-1925.

Mullen, K. M., Vohr, B. R., Katz, K. H., Schneider, K. C., Lacadie, C., Hampson, M., et al. (2010). Preterm birth results in alterations in neural connectivity at age 16 years. *Neuroimage*.

Neil, J., Miller, J., Mukherjee, P., & Huppi, P. S. (2002). Diffusion tensor imaging of normal and injured developing human brain - a technical review. *NMR Biomed, 15*(7-8), 543-552.

O'Leary-Moore, S., Parnell, S. E., Lipinski, R. J., & Sulik, K. K. (2011). Magnetic resonance-based imaging in animal models of fetal alcohol spectrum disorders. *Neuropsychology Review, 21(2)*, in press.

Pantoni, L., & Garcia, J. H. (1995). The significance of cerebral white matter abnormalities 100 years after Binswanger's report. A review. *Stroke, 26*(7), 1293-1301.

Paus, T. (2009). Growth of white matter in the adolescent brain: Myelin or axon? *Brain Cogn*.

Perham-Hester, K. A., & Gessner, B. D. (1997). Correlates of drinking during the third trimester of pregnancy in Alaska. *Matern Child Health J, 1*(3), 165-172.

Pfefferbaum, A., Sullivan, E. V., Hedehus, M., Adalsteinsson, E., Lim, K. O., & Moseley, M. (2000). In vivo detection and functional correlates of white matter microstructural disruption in chronic alcoholism. *Alcohol Clin Exp Res, 24*(8), 1214-1221.

Qiu, D., Tan, L. H., Zhou, K., & Khong, P. L. (2008). Diffusion tensor imaging of normal white matter maturation from late childhood to young adulthood: voxel-wise evaluation of mean diffusivity, fractional anisotropy, radial and axial diffusivities, and correlation with reading development. *Neuroimage, 41*(2), 223-232.

Radua, J., Via, E., Catani, M., & Mataix-Cols, D. (2010). Voxel-based meta-analysis of regional white-matter volume differences in autism spectrum disorder versus healthy controls. *Psychological Medicine*, 1-12.

Raichle, M. E., MacLeod, A. M., Snyder, A. Z., Powers, W. J., Gusnard, D. A., & Shulman, G. L. (2001). A default mode of brain function. *Proc Natl Acad Sci U S A, 98*(2), 676-682.

Raichle, M. E., & Snyder, A. Z. (2007). A default mode of brain function: a brief history of an evolving idea. *Neuroimage, 37*(4), 1083-1090; discussion 1097-1089.

Rao, S. M. (1995). Neuropsychology of multiple sclerosis. *Curr Opin Neurol, 8*(3), 216-220.

Riley, E. P., Mattson, S. N., Sowell, E. R., Jernigan, T. L., Sobel, D. F., & Jones, K. L. (1995). Abnormalities of the corpus callosum in children prenatally exposed to alcohol. *Alcohol Clin Exp Res, 19*(5), 1198-1202.

Roebuck, T. M., Mattson, S. N., & Riley, E. P. (2002). Interhemispheric transfer in children with heavy prenatal alcohol exposure. *Alcohol Clin Exp Res, 26*(12), 1863-1871.

Sampson, P. D., Streissguth, A. P., Bookstein, F. L., Little, R. E., Clarren, S. K., Dehaene, P., et al. (1997). Incidence of fetal alcohol syndrome and prevalence of alcohol-related neurodevelopmental disorder. *Teratology, 56*(5), 317-326.

Schmithorst, V. J., & Yuan, W. (2009). White matter development during adolescence as shown by diffusion MRI. *Brain Cogn*.

Schweder, P. M., Joint, C., Hansen, P. C., Green, A. L., Quaghebeur, G., & Aziz, T. Z. (2010). Chronic pedunculopontine nucleus stimulation restores functional connectivity. *Neuroreport, 21*(17), 1065-1068.

Shukla, D. K., Keehn, B., & Muller, R. A. (2010). Tract-specific analyses of diffusion tensor imaging show widespread white matter compromise in autism spectrum disorder. *Journal of Child Psychology and Psychiatry and Allied Disciplines*.

Skudlarski, P., Jagannathan, K., Calhoun, V. D., Hampson, M., Skudlarska, B. A., & Pearlson, G. (2008). Measuring brain connectivity: diffusion tensor imaging validates resting state temporal correlations. *Neuroimage, 43*(3), 554-561.

Smith, S. M., Jenkinson, M., Johansen-Berg, H., Rueckert, D., Nichols, T. E., Mackay, C. E., et al. (2006). Tract-based spatial statistics: voxelwise analysis of multi-subject diffusion data. *Neuroimage, 31*(4), 1487-1505.

Sowell, E. R., Johnson, A., Kan, E., Lu, L. H., Van Horn, J. D., Toga, A. W., et al. (2008). Mapping white matter integrity and neurobehavioral correlates in children with fetal alcohol spectrum disorders. *J Neurosci, 28*(6), 1313-1319.

Sowell, E. R., Mattson, S. N., Thompson, P. M., Jernigan, T. L., Riley, E. P., & Toga, A. W. (2001). Mapping callosal morphology and cognitive correlates: Effects of heavy prenatal alcohol exposure. *Neurology, 57*(2), 235-244.

Sowell, E. R., Thompson, P. M., Mattson, S. N., Tessner, K. D., Jernigan, T. L., Riley, E. P., et al. (2001). Voxel-based morphometric analyses of the brain in children and adolescents prenatally exposed to alcohol. *Neuroreport, 12*(3), 515-523.

Stejskal, E. O., & Tanner, J. E. (1965). Spin diffusion measurements: spin echos in the presence of time-dependent field gradient. *J. Chem Phys, 42*, 288-292.

Streissguth, A. P., Sampson, P. D., Olson, H. C., Bookstein, F. L., Barr, H. M., Scott, M., et al. (1994). Maternal drinking during pregnancy: attention and short-term memory in 14-year-old offspring--a longitudinal prospective study. *Alcohol Clin Exp Res, 18*(1), 202-218.

Sullivan, E. V. (Ed.). (2010). *Historical Feature on Disconnexion Syndrome in Animals and Man by Norman Geschwind [Special Issue]. Neuropsychology Review* (Vol. 20(2)).

Sullivan, E. V., & Pfefferbaum, A. (2011). Diffusion tensor imaging in aging and age-related disorders. In D. K. Jones (Ed.), *Diffusion MRI: Theory, Methods, and Applications* (pp. 624-643). Oxford: Oxford University Press.

Teipel, S. J., Meindl, T., Wagner, M., Stieltjes, B., Reuter, S., Hauenstein, K. H., et al. (2010). Longitudinal Changes in Fiber Tract Integrity in Healthy Aging and Mild Cognitive Impairment: A DTI Follow-Up Study. *J Alzheimers Dis, 22*(2), 507-522.

Trivedi, R., Gupta, R. K., Shah, V., Tripathi, M., Rathore, R. K., Kumar, M., et al. (2008). Treatment-induced plasticity in cerebral palsy: a diffusion tensor imaging study. *Pediatric Neurology, 39*(5), 341-349.

Uddin, L. Q., Kelly, A. M., Biswal, B. B., Margulies, D. S., Shehzad, Z., Shaw, D., et al. (2008). Network homogeneity reveals decreased integrity of default-mode network in ADHD. *J Neurosci Methods, 169*(1), 249-254.

Utsunomiya, H. (2010). Diffusion MRI abnormalities in pediatric neurological disorders. *Brain and Development*.

Walhovd, K. B., Westlye, L. T., Moe, V., Slinning, K., Due-Tonnessen, P., Bjornerud, A., et al. (2010). White matter characteristics and cognition in prenatally opiate- and polysubstance-exposed children: a diffusion tensor imaging study. *AJNR Am J Neuroradiol, 31*(5), 894-900.

Warner, T. D., Behnke, M., Eyler, F. D., Padgett, K., Leonard, C., Hou, W., et al. (2006). Diffusion tensor imaging of frontal white matter and executive functioning in cocaine-exposed children. *Pediatrics, 118*(5), 2014-2024.

Wilde, E. A., Chu, Z., Bigler, E. D., Hunter, J. V., Fearing, M. A., Hanten, G., et al. (2006). Diffusion tensor imaging in the corpus callosum in children after moderate to severe traumatic brain injury. *J Neurotrauma, 23*(10), 1412-1426.

Wozniak, J. R., Krach, L., Ward, E., Mueller, B. A., Muetzel, R., Schnoebelen, S., et al. (2007). Neurocognitive and neuroimaging correlates of pediatric traumatic brain injury: a diffusion tensor imaging (DTI) study. *Arch Clin Neuropsychol, 22*(5), 555-568.

Wozniak, J. R., Mueller, B. A., Chang, P., Muetzel, R. L., Caros, L., & Lim, K. O. (2006). Diffusion Tensor Imaging in Children with Fetal Alcohol Spectrum Disorders. *Alcoholism, Clinical and Experimental Research, 30*(10), 1799-1806.

Wozniak, J. R., Mueller, B. A., & Lim, K. O. (2008). Diffusion Tensor Imaging. In C. A. Nelson & M. Luciana (Eds.), *Handbook of Developmental Cognitive Neuroscience - Second Edition* (pp. 301-310). Cambridge, MA: MIT Press.

Wozniak, J. R., Mueller, B. A., Muetzel, R. L., Bell, C. J., Hoecker, H. L., Nelson, M. L., et al. (in press). Inter-hemispheric functional connectivity disruption in children with prenatal alcohol exposure. *Alcoholism, Clinical and Experimental Research*.

Wozniak, J. R., Mueller, B. A., Ward, E. E., Lim, K. O., & Day, J. W. (in press). White matter abnormalities and neurocognitive correlates in children and adolescents with myotonic dystrophy type 1: A Diffusion Tensor Imaging study. *Neuromuscular Disorders*.

Wozniak, J. R., Muetzel, R. L., Mueller, B. A., McGee, C. L., Freerks, M. A., Ward, E. E., et al. (2009). Microstructural corpus callosum anomalies in children with prenatal alcohol exposure: an extension of previous diffusion tensor imaging findings. *Alcoholism, Clinical and Experimental Research, 33*(10), 1825-1835.

Wu, T. C., Wilde, E. A., Bigler, E. D., Li, X., Merkley, T. L., Yallampalli, R., et al. (2010). Longitudinal Changes in the Corpus Callosum following Pediatric Traumatic Brain Injury. *Developmental Neuroscience*.

Yakolev, P. I., & Lecours, A. R. (1967). The myelogenic cycles of regional maturation of the brain. In A. Minkowski (Ed.), *Regional development of the brain in early life* (pp. 3-70). Blackwell: Oxford.

Yoshida, S., Hayakawa, K., Yamamoto, A., Okano, S., Kanda, T., Yamori, Y., et al. (2010). Quantitative diffusion tensor tractography of the motor and sensory tract in children with cerebral palsy. *Developmental Medicine and Child Neurology*.